

# Wiskott–Aldrich syndrome protein (WASP) is a tumor suppressor in T cell lymphoma

Matteo Menotti<sup>1,13</sup>, Chiara Ambrogio<sup>2,15</sup>, Taek-Chin Cheong<sup>3,15</sup>, Chiara Pighi<sup>1,3</sup>, Ines Mota<sup>1</sup>, Seth H. Cassel<sup>4,5,6,7</sup>, Mara Compagno<sup>1,3</sup>, Qi Wang<sup>3</sup>, Riccardo Dall'Olio<sup>1</sup>, Valerio G. Minero<sup>1</sup>, Teresa Poggio<sup>1</sup>, Geeta Geeta Sharma<sup>8</sup>, Enrico Patrucco<sup>1</sup>, Cristina Mastini<sup>1</sup>, Ramesh Choudhari<sup>1,14</sup>, Achille Pich<sup>1</sup>, Alberto Zamo<sup>9</sup>, Roberto Piva<sup>1</sup>, Silvia Giliani<sup>10</sup>, Luca Mologni<sup>8</sup>, Clayton K. Collings<sup>4,5</sup>, Cigall Kadoch<sup>4,5</sup>, Carlo Gambacorti-Passerini<sup>8</sup>, Luigi D. Notarangelo<sup>11</sup>, Ines M. Anton<sup>12</sup>, Claudia Voena<sup>1\*</sup> and Roberto Chiarle<sup>1,3\*</sup>

**In T lymphocytes, the Wiskott–Aldrich Syndrome protein (WASP) and WASP-interacting-protein (WIP) regulate T cell antigen receptor (TCR) signaling, but their role in lymphoma is largely unknown. Here we show that the expression of WASP and WIP is frequently low or absent in anaplastic large cell lymphoma (ALCL) compared to other T cell lymphomas. In anaplastic lymphoma kinase-positive (ALK+) ALCL, WASP and WIP expression is regulated by ALK oncogenic activity via its downstream mediators STAT3 and C/EBP- $\beta$ . ALK+ lymphomas were accelerated in WASP- and WIP-deficient mice. In the absence of WASP, active GTP-bound CDC42 was increased and the genetic deletion of one CDC42 allele was sufficient to impair lymphoma growth. WASP-deficient lymphoma showed increased mitogen-activated protein kinase (MAPK) pathway activation that could be exploited as a therapeutic vulnerability. Our findings demonstrate that WASP and WIP are tumor suppressors in T cell lymphoma and suggest that MAP-kinase kinase (MEK) inhibitors combined with ALK inhibitors could achieve a more potent therapeutic effect in ALK+ ALCL.**

Loss-of-function mutations in the *WAS* gene, which encodes WASP, causes Wiskott–Aldrich syndrome (WAS), a rare X-linked primary immunodeficiency of variable severity characterized by microthrombocytopenia, eczema, autoimmunity, recurrent infections and a predisposition to lymphoma development<sup>1</sup>. As WASP is selectively expressed in hematopoietic cells, the phenotype in patients with WAS is associated with defects in hematopoiesis and the immune system. WASP abundance in cells is regulated by WIP. WIP, encoded by the gene *WIPF1*, binds to the WH1 domain of WASP and protects WASP from degradation<sup>2–5</sup>. The main regulator of WASP activation is the Rho family GTPase cell division cycle 42 (CDC42). In its GTP-bound state, CDC42 binds the GTPase-binding domain of WASP to release the verprolin homology domain–cofilin homology domain–acidic region autoinhibitory domain and to permit the binding to the actin-related protein–2/3 (ARP2/3) complex and actin nucleation<sup>4,6,7</sup>. Additional mediators, such as PIP2, and hematopoietic-specific kinases, such as BTK, LTK, FYN and NCK1, contribute to the activation of WASP<sup>7,8</sup>.

T lymphocytes from patients with WAS and WASP- and WIP-deficient mice show a number of defects, including defective proliferation in response to T cell receptor (TCR) stimulation, disturbed formation of surface projections, defective cytokine polarization

and secretion, disrupted assembly of filamentous actin at the immunological synapse and impaired TCR-mediated signaling<sup>7–10</sup>. Other cells of the adaptive immune system, such as B cells, as well as cells of the innate immune system, such as macrophages and dendritic cells, also have functional defects that have yet to be completely characterized<sup>7,11</sup>. Importantly, WASP-dependent actin nucleation is essential for the formation of the immunological synapses in T cells and several other WASP-mediated phenotypes<sup>4,7</sup>.

Increasing evidence supports the concept that TCR-mediated signaling is also critical for the pathology of T cell lymphoma. Mutations in genes involved in TCR signaling, such as *KRAS*, *RHOA*, *VAV1*, *CD28*, *FYN*, *LCK* and *PLCG1*, are frequently found in T cell lymphomas that retain TCR expression, such as peripheral T cell lymphoma (PTCL-NOS) and angioimmunoblastic T cell lymphoma (AITL)<sup>12</sup>. By contrast, in ALCL, TCR signaling is typically lost and is bypassed by oncogenic tyrosine kinase signaling, most often secondary to aberrant activation of ALK, ROS1 or TYK2<sup>13–16</sup>. Recent discoveries have highlighted, among several pathways downstream of TCR signaling, the pathogenetic role of Rho GTPases, such as RAC1, CDC42 and RHOA, in T cell lymphoma<sup>12</sup>. Inactivating or dominant negative mutations in *RHOA* are the

<sup>1</sup>Department of Molecular Biotechnology and Health Sciences, University of Torino, Torino, Italy. <sup>2</sup>Department of Medical Oncology, Dana-Farber Cancer Institute, Boston, MA, USA. <sup>3</sup>Department of Pathology, Boston Children's Hospital and Harvard Medical School, Boston, MA, USA. <sup>4</sup>Department of Pediatric Oncology, Dana-Farber Cancer Institute and Harvard Medical School, Boston, MA, USA. <sup>5</sup>The Broad Institute of MIT and Harvard, Cambridge, MA, USA. <sup>6</sup>Biomedical and Biological Sciences Program, Harvard Medical School, Boston, MA, USA. <sup>7</sup>Medical Scientist Training Program, Harvard Medical School, Boston, MA, USA. <sup>8</sup>School of Medicine and Surgery, University of Milan-Bicocca, Monza, Italy. <sup>9</sup>Department of Oncology, University of Torino, Torino, Italy. <sup>10</sup>Nocivelli Institute for Molecular Medicine, Department of Molecular and Translational Medicine, University of Brescia, Brescia, Italy. <sup>11</sup>Laboratory of Clinical Immunology and Microbiology, National Institute of Allergy and Infectious Diseases, National Institutes of Health, Bethesda, MD, USA. <sup>12</sup>Department of Molecular and Cellular Biology, Centro Nacional de Biotecnología (CNB-CSIC), Madrid, Spain. <sup>13</sup>Present address: Cell Signalling Group, Cancer Research UK Manchester Institute, University of Manchester, Manchester, UK. <sup>14</sup>Present address: Center of Emphasis in Cancer, Paul L. Foster School of Medicine, Department of Biomedical Sciences, Texas Tech University Health Sciences Center, El Paso, TX, USA. <sup>15</sup>These authors contributed equally: Chiara Ambrogio, Taek-Chin Cheong. \*e-mail: [claudia.voena@unito.it](mailto:claudia.voena@unito.it); [roberto.chiarle@childrens.harvard.edu](mailto:roberto.chiarle@childrens.harvard.edu)

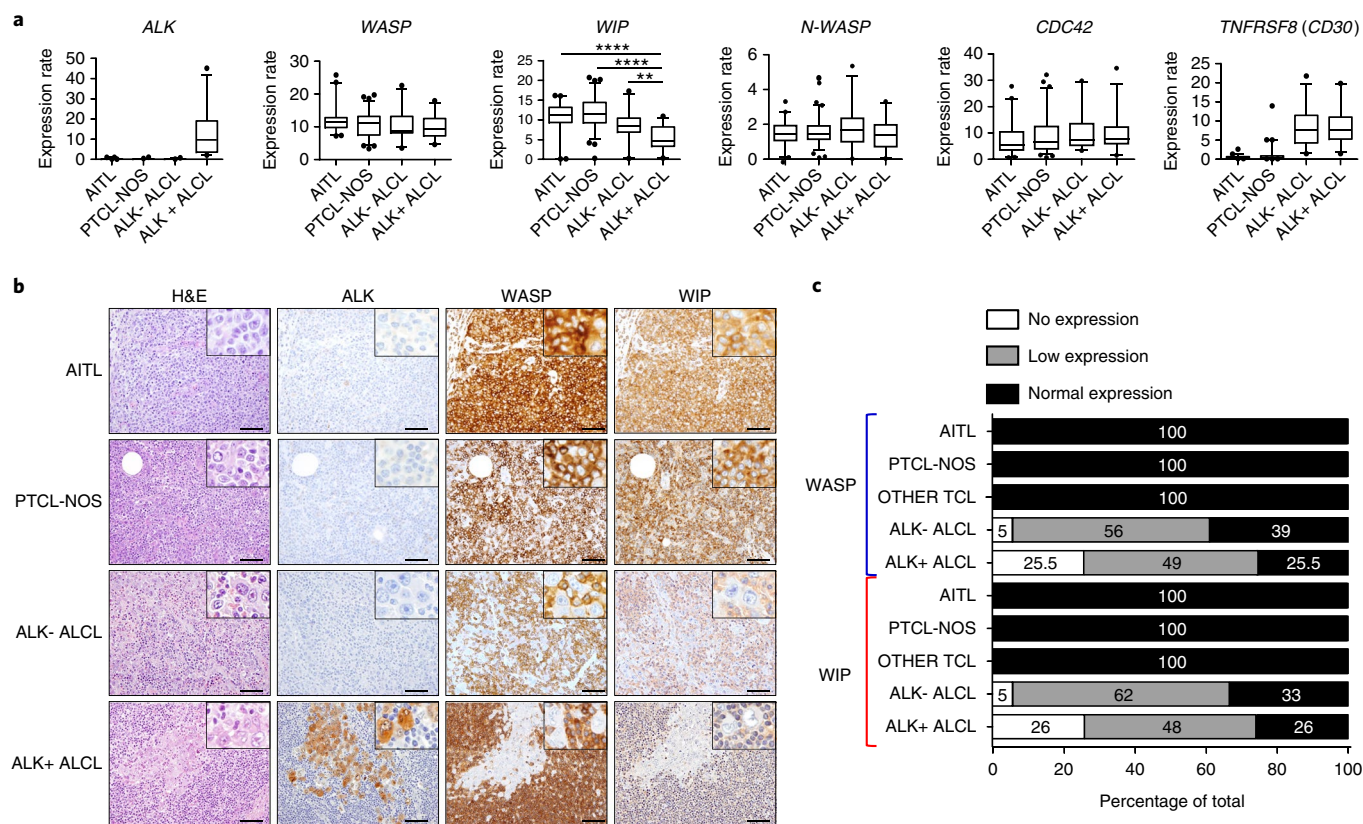


**Fig. 1 | *WASP* and *WIP* are selectively down-regulated in ALCL. a**, Gene-expression profiling analysis of *ALK*, *WASP*, *WIP*, *N-WASP*, *CDC42* and *TNFRSF8 (CD30)* on different cases of human T cell lymphomas: AITL,  $n=40$ ; PTCL-NOS,  $n=74$ ; ALK- ALCL,  $n=24$ ; ALK+ ALCL,  $n=30$ . The boxes represent the first and third quartiles and the line represents the median. The whiskers represent the upper and lower limits of the range (ALK+ ALCL versus AITL,  $***P=5.85 \times 10^{-6}$ ; ALK+ ALCL versus PTCL-NOS,  $****P=6.08 \times 10^{-12}$ ; ALK+ ALCL versus ALK- ALCL,  $**P=0.0075$ ; significance was determined by unpaired, two-tailed Student's *t*-test). *TNFRSF8 (CD30)* is strongly expressed in ALK- and ALK+ ALCL but not in other TCL subtypes. **b**, Representative H&E staining and immunohistochemistry stainings performed with the indicated antibody on human T cell lymphoma subtypes. The number of human T cell lymphoma samples analyzed is reported in Fig. 1c. *WASP* antibody was validated in formalin-fixed samples with inducible *WASP* expression (Supplementary Fig. 7f). *WIP* antibody cross reacts with mouse *WIP* and was validated on *WIP* knockout cells (Supplementary Fig. 1b). Scale bar, 100  $\mu$ m. Insets: high-magnification images. **c**, *WASP* and *WIP* expression in human T cell lymphoma subtypes. AITL,  $n=20$ ; PTCL-NOS,  $n=20$ ; ALK- ALCL,  $n=29$ ; ALK+ ALCL,  $n=43$  for *WASP* and  $n=31$  for *WIP*; other TCL are natural killer (NK)/T cell lymphoma, nasal-type,  $n=3$  and hepatosplenic  $\gamma\delta$  T cell lymphoma,  $n=3$ . The number of patient samples is indicated for each lymphoma subtype. *WASP* and *WIP* expressions were quantified by immunostaining. Normal expression, expression equal to surrounding reactive T cells; low expression, decreased expression compared to surrounding reactive T cells; and no expression, absence of expression in lymphoma cells.

most common recurrent genetic event in AITL and are also present in PTCL-NOS<sup>17–19</sup>. *RAC1* and *CDC42* genes are not recurrently mutated in lymphoma, yet they are activated by mutations of upstream GTP-exchange factors (GEFs), such as *VAV1* and *VAV3*. *VAV1* is frequently activated by mutations and translocations in PTCL<sup>20</sup>, whereas oncogenic *ALK* constitutively activates *VAV1* and *VAV3* in ALCL, thereby increasing *RAC1* and *CDC42* activity and promoting lymphoma survival<sup>21–23</sup>. Taken together, these studies indicate there is a critical role of downstream mediators of TCR signaling and Rho GTPases in T cell lymphoma. In this context, in contrast to the well-characterized function of *WASP* and *WIP* in normal TCR signaling, their role in T cell lymphoma is largely unknown.

We investigated *WASP* and *WIP* expression in a series of T cell lymphomas and found that *WASP* and *WIP* expression are selectively low or absent in ALCL but retained in lymphomas with conserved TCR signaling, such as PTCL-NOS and AITL. *WASP* or *WIP* deficiency significantly accelerated the development of ALK-driven lymphoma in mice by increasing active *CDC42* and enhancing MAPK signaling. Reduction of *CDC42* abundance by deletion of one copy of *Cdc42* abrogated the acceleration of lymphomagenesis in *WASP*-deficient mice. Therapeutically, the forced re-expression

of *WASP* impaired lymphoma growth, and MAPK inhibitors potentiated the effect of the ALK inhibitor crizotinib and exposed an enhanced vulnerability in ALK-driven lymphoma. Overall, these results indicate that *WASP* is a tumor suppressor in ALCL and high-light specific therapeutic susceptibilities.

## Results

**Selective low expression of *WASP* and *WIP* in ALCL.** To investigate the potential role of *WASP* and *WIP* in the ontogeny of T cell lymphomas, we analyzed *WASP* and *WIP* mRNA expression in a series of human T cell lymphomas, including AITL, PTCL-NOS, ALK+ and ALK-negative (ALK-) ALCL, which altogether account for more than 90% of T cell lymphomas<sup>24</sup>. *ALK* expression was confined to ALK+ ALCL, *TNFRSF8 (CD30)* expression was enriched in ALCL; *WASP*, *CDC42* and *WASL (N-WASP)* mRNA expression was similar in various subtypes of T cell lymphoma, whereas *WIP* mRNA was significantly lower in ALCL and lowest in ALK+ ALCL (Fig. 1a). Considering that *WIP* regulates *WASP* stability, we investigated the expression of *WASP* and *WIP* proteins by immunohistochemistry in a series of T lymphomas. We found that expression of *WASP* and *WIP* was frequently low or negative in ALCL, but it was always retained in

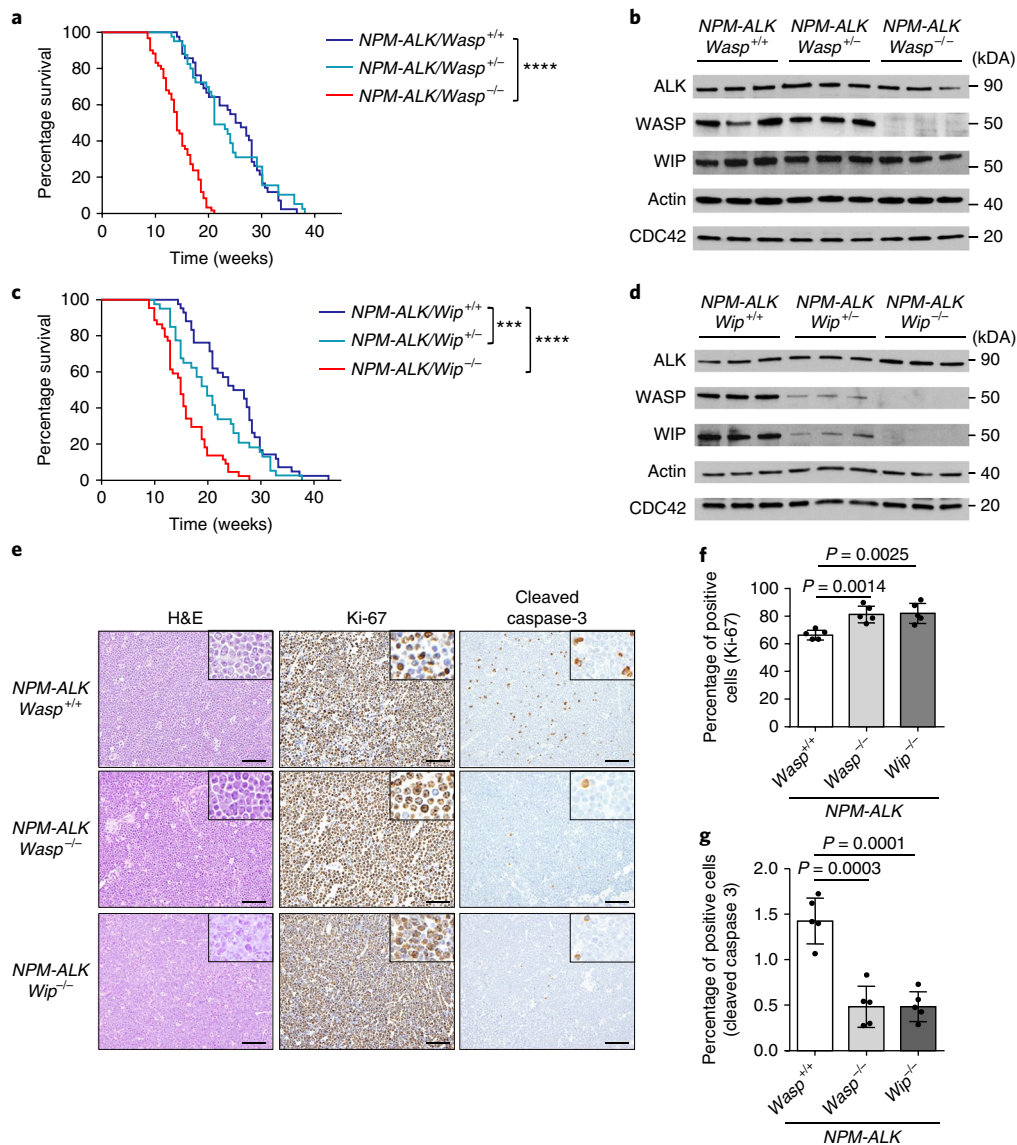


**Fig. 2 | WASP is an oncosuppressor in ALK+ T cell lymphoma.** **a**, Kaplan–Meier analysis of overall survival of *NPM-ALK* transgenic mice crossed with WASP-deficient mice (blue, *NPM-ALK/Wasp<sup>+/+</sup>*,  $n = 35$ ; light blue, *NPM-ALK/Wasp<sup>+/-</sup>*,  $n = 37$ ; red, *NPM-ALK/Wasp<sup>-/-</sup>*,  $n = 30$ ). The number of mice for each genotype is indicated. *NPM-ALK/Wasp<sup>+/+</sup>* versus *NPM-ALK/Wasp<sup>-/-</sup>*, \*\*\*\* $P < 0.0001$ ; significance was determined by log-rank (Mantel–Cox) test. **b**, Western blot analysis from  $n = 3$  independent primary lymphomas isolated from *NPM-ALK* transgenic mice crossed with WASP-deficient mice. The blot is representative of at least two independent experiments with similar results. Actin was used as a loading control. Uncropped blots are available in Supplementary Fig. 11. **c**, Kaplan–Meier analysis of overall survival of *NPM-ALK* transgenic mice crossed with WIP-deficient mice (blue, *NPM-ALK/Wip<sup>+/+</sup>*,  $n = 26$ ; light blue, *NPM-ALK/Wip<sup>+/-</sup>*,  $n = 32$ ; red, *NPM-ALK/Wip<sup>-/-</sup>*,  $n = 30$ ). The number of mice for each genotype is indicated. *NPM-ALK/Wip<sup>+/+</sup>* versus *NPM-ALK/Wip<sup>-/-</sup>*, \*\*\*\* $P = 0.0044$ ; *NPM-ALK/Wip<sup>+/+</sup>* versus *NPM-ALK/Wip<sup>+/-</sup>*, \*\*\*\* $P < 0.0001$ ; significance was determined by log-rank (Mantel–Cox) test. **d**, Western blot analysis from  $n = 3$  independent primary lymphomas isolated from *NPM-ALK* transgenic mice crossed with WIP-deficient mice. The blot is representative of at least two independent experiments with similar results. Actin was used as a loading control. Uncropped blots are available in Supplementary Fig. 11. **e**, Representative H&E stain (left) and immunohistochemistry for Ki-67 (middle) and cleaved Caspase 3 (right), performed on *NPM-ALK* lymphoma with the indicated genotypes ( $n = 5$  mice for each genotype). Scale bar, 100  $\mu\text{m}$ . Insets: high-magnification images. **f, g**, Quantification of Ki-67 (**f**) and cleaved caspase 3 (**g**) positive cells in *NPM-ALK* lymphoma with the indicated genotypes ( $n = 5$  mice for each genotype). Data are shown as means  $\pm$  s.d.; significance was determined by an unpaired, two-tailed Student’s *t*-test.

AITL and PTCL-NOS as well as in other rare T cell lymphoma, such as natural killer (NK)/T cell lymphoma and  $\gamma\delta$  hepatosplenic T cell lymphoma (Fig. 1b,c and Supplementary Fig. 1a,b). Taken together, these data showed that WASP and WIP expression is selectively decreased in ALCL as compared to other T cell lymphomas.

**WASP or WIP deficiencies accelerate T cell lymphoma development.** WASP-deficient mice do not develop lymphoma spontaneously and have normal T thymic cell maturation, but they exhibit

defective T cell activation<sup>9</sup>. To directly address the biological role of WASP and WIP in ALCL, we crossed *NPM-ALK* transgenic mice with *Wasp<sup>-/-</sup>* mice. The *NPM-ALK* fusion protein is the canonical and most frequent driver oncogene in ALCL, and *NPM-ALK* transgenic mice develop T cell lymphoma with high penetrance<sup>25</sup>. *NPM-ALK/Wasp<sup>-/-</sup>* females and *NPM-ALK/Wasp<sup>-/-</sup>* males showed similar phenotypes and are collectively referred to as *NPM-ALK/Wasp<sup>-/-</sup>* mice. As expected, *NPM-ALK/Wasp<sup>-/-</sup>* mice had a complete lack of WASP (Supplementary Fig. 1c). The number of T cells and the pattern of

thymic T cell development were comparable in *NPM-ALK* and *NPM-ALK/Wasp<sup>-/-</sup>* mice (Supplementary Fig. 1d,e). Remarkably, WASP deficiency significantly accelerated the onset of lymphomas and hastened mortality (Fig. 2a,b). *NPM-ALK/Wasp<sup>+/-</sup>* female mice had protein abundance comparable to *NPM-ALK/Wasp<sup>+/+</sup>* mice and did not show any acceleration in lymphomagenesis (Fig. 2a,b).

Mice with WIP deficiency have impaired T and B cell activation as a result of defects in the subcortical actin filament network. WASP is almost undetectable in *Wip<sup>-/-</sup>* mice because WASP stability depends on binding to WIP<sup>2</sup>. Recently, patients with disruptive mutations in *WIP* have been identified. These patients lack expression of both WIP and WASP and present with a clinical phenotype similar to patients with WAS<sup>26,27</sup>. Therefore, we reasoned that if the amount of WASP protein is critical for the kinetics of NPM-ALK-driven lymphoma, WIP deficiency should accelerate lymphomagenesis in a manner similar to WASP deficiency. Indeed, *NPM-ALK/Wip<sup>-/-</sup>* mice phenocopied *NPM-ALK/Wasp<sup>-/-</sup>* mice with regard to the onset of lymphoma. In contrast to *NPM-ALK/Wasp<sup>+/-</sup>* mice, *NPM-ALK/Wip<sup>+/-</sup>* mice had a phenotype intermediate between *NPM-ALK/Wip<sup>-/-</sup>* and *NPM-ALK/Wip<sup>+/+</sup>* mice (Fig. 2c). When we analyzed the protein levels, as expected, *NPM-ALK/Wip<sup>-/-</sup>* lymphomas had undetectable levels of both WIP and WASP<sup>3</sup>, whereas *NPM-ALK/Wip<sup>+/-</sup>* lymphomas expressed intermediate levels of both WIP and WASP (Fig. 2d). Immunostains for cleaved caspase 3 and Ki-67 protein demonstrated that the accelerated lymphomagenesis in *NPM-ALK/Wasp<sup>-/-</sup>* or *NPM-ALK/Wip<sup>-/-</sup>* mice was associated with reduced apoptosis and increased proliferation of lymphoma cells (Fig. 2e–g). The similarity of the survival phenotype between WASP and WIP-deficient mice (Fig. 2a–c) is consistent with the near complete absence of WASP in WIP-deficient mice (Fig. 2d) and is in keeping with the known role of WIP in WASP stability<sup>3</sup>. Heterozygous *Wip<sup>+/-</sup>* mice had intermediate levels of WASP and WIP expression as well as an intermediate survival phenotype, indicating that relative levels of WASP can contribute to the kinetics of lymphoma development. Overall, these data suggest that WASP deficiency probably bears responsibility for the phenotype in WIP-deficient mice. These results mirror the findings in human patients with WAS, in whom a complete absence of the protein is associated with a more profound phenotype, including a higher risk of lymphoma development, compared to patients that retain partial expression of WASP and present with milder phenotypes and a lower incidence of lymphoid malignancies<sup>10,28</sup>.

Oncogenic activity of NPM-ALK in lymphocytes controls actin polymerization via a direct activation of VAV1 and VAV3, which are GEFs for RAC1 and CDC42<sup>21,22</sup>. Lymphocytes transformed by NPM-ALK are large and irregular (hence the term ‘anaplastic’ that collectively defines ALK-rearranged lymphoma), hypermotile and have accentuated cellular polarization due to polar assembly of actin filaments<sup>21,23</sup>. Lymphomas that developed in *NPM-ALK/Wasp<sup>-/-</sup>* or *NPM-ALK/Wip<sup>-/-</sup>* mice had a significantly smaller mean cellular diameter than *NPM-ALK* lymphoma cells (Supplementary Fig. 2a,b). *NPM-ALK/Wasp<sup>-/-</sup>* or *NPM-ALK/Wip<sup>-/-</sup>* lymphoma cells also showed markedly decreased actin polarization (Supplementary Fig. 2a,c), consistent with defects of actin nucleation and assembly associated with complete loss of WASP or WIP. In reverse experiments, doxycycline-inducible overexpression of WASP and WIP in human ALCL resulted in increased mean cellular diameter and actin polymerization (Supplementary Fig. 2d,e).

**CDC42 mediates accelerated lymphoma development in WASP-deficient cells.** To elucidate the mechanisms of accelerated lymphomagenesis in the absence of WASP, we characterized the expression profiles of *NPM-ALK-Wasp<sup>-/-</sup>* lymphomas (Supplementary Fig. 3a). Gene set enrichment analysis demonstrated that serum response factor pathway, known to be activated by Rho family GTPase signaling<sup>29</sup>, as well as other GTPase signatures, were significantly

enriched in *NPM-ALK/Wasp<sup>-/-</sup>* lymphoma compared to *NPM-ALK/Wasp<sup>+/+</sup>* lymphoma (Supplementary Fig. 3b–d). Since WASP is a critical substrate of GTP-bound CDC42, we reasoned that WASP deficiency could affect CDC42 activity in lymphoma cells, resulting in an increased GTPase signature. To explore this possibility, we assessed the abundance of active GTP-bound CDC42 in *NPM-ALK/Wasp<sup>-/-</sup>* lymphoma. We analyzed *NPM-ALK/Wasp<sup>-/-</sup>* and *NPM-ALK/Wasp<sup>+/+</sup>* lymphomas by CDC42-specific GTPase assay. *NPM-ALK/Wasp<sup>-/-</sup>* lymphomas had significantly higher levels of GTP-bound CDC42 than *NPM-ALK/Wasp<sup>+/+</sup>* lymphomas (Fig. 3a), indicating that the amount of active CDC42 is increased in cells that lack WASP. In addition to increased CDC42 activation, *NPM-ALK/Wasp<sup>-/-</sup>* lymphomas also showed increased activation of the MAPK pathway as assessed by ERK1/2 phosphorylation (Fig. 3b).

To assess directly whether CDC42 abundance was critical for lymphoma acceleration in WASP-deficient cells, we crossed *NPM-ALK/Wasp<sup>-/-</sup>* mice with a conditional *Cdc42<sup>lox</sup>* allele; deletion of *Cdc42* in T cells was accomplished by further crossing with *CD4-Cre* mice<sup>23</sup>. The deletion of one *Cdc42* allele was associated with decreased protein abundance (Fig. 3c) and was sufficient to delay lymphoma development in *NPM-ALK/Wasp<sup>-/-</sup>* mice (Fig. 3d). Remarkably, lymphoma development and survival of *NPM-ALK/Wasp<sup>-/-</sup>/Cdc42<sup>+/+</sup>/CD4-Cre* mice was similar to *NPM-ALK/Wasp<sup>+/+</sup>* mice. *NPM-ALK/Wasp<sup>-/-</sup>* mice with a complete knockout of *Cdc42* (*NPM-ALK/Wasp<sup>-/-</sup>/Cdc42<sup>0/0</sup>/CD4-Cre* mice) died prematurely because of multiorgan failure due to an inflammatory infiltrate, and so the development of lymphoma could not be assessed. Apoptosis was uniformly higher and proliferation consistently lower in *NPM-ALK/Wasp<sup>-/-</sup>/Cdc42<sup>+/+</sup>/CD4-Cre* lymphomas than in *NPM-ALK/Wasp<sup>-/-</sup>* lymphomas but was comparable to *NPM-ALK/Wasp<sup>+/+</sup>* lymphomas (Fig. 3e–g). We conclude that the accelerated lymphomagenesis in *NPM-ALK/Wasp<sup>-/-</sup>* mice depends on the abundance of CDC42.

To further characterize the role of CDC42 in *NPM-ALK/Wasp<sup>-/-</sup>* lymphomas, we immortalized lymphoma cell lines of different genotypes and induced *Cdc42* deletion with a tamoxifen-inducible Cre-recombinase. As expected, deletion of one *Cdc42* allele reduced CDC42 protein abundance by approximately 50%, whereas biallelic deletion abrogated CDC42 expression (Fig. 4a). Deletion of one *Cdc42* allele significantly impaired the growth of *NPM-ALK/Wasp<sup>-/-</sup>* lymphoma cells but not of *NPM-ALK/Wasp<sup>+/+</sup>* lymphoma cells (Fig. 4b), mirroring the results obtained in mice (Fig. 3d) and confirming that CDC42 abundance is critical for *Wasp<sup>-/-</sup>* lymphoma. Consistently, deletion of one *Cdc42* allele produced an increase in apoptosis in *NPM-ALK/Wasp<sup>-/-</sup>* lymphomas but not in *NPM-ALK/Wasp<sup>+/+</sup>* lymphoma cells (Fig. 4c). Consistent with our previous findings<sup>23</sup>, in *NPM-ALK/Wasp<sup>+/+</sup>* lymphoma only the biallelic deletion of *Cdc42* induced impairment of lymphoma growth and apoptosis (Fig. 4c). Altogether, these data demonstrate that WASP-deficient cells are exquisitely sensitive to the cellular abundance of CDC42.

**Oncogenic ALK activity promotes WASP and WIP downregulation via STAT3 and C/EBP-β.** To investigate WASP- and WIP-dependent mechanisms of ALK+ ALCL lymphoma progression, we measured WASP and WIP expression in ALK cell lines and confirmed that in several cell lines they were lower than in normal T cells or other lymphoma types (Fig. 5a and Supplementary Fig. 4a). By contrast, N-WASP was not decreased in ALCL (Supplementary Fig. 5a). *WIP* mRNA was lower in ALK+ ALCL cell lines than in other T cell lines or in T cells from normal donors, whereas *WASP* mRNA was more variable (Fig. 5b). Overall, these patterns of gene expression in ALCL cell lines recapitulate the findings in primary ALCL from patients (Fig. 1).

As it is known that ALK oncogenic activity controls protein expression by transcriptional regulation or epigenetic silencing<sup>30,31</sup>, we tested whether WASP and WIP expression were directly controlled

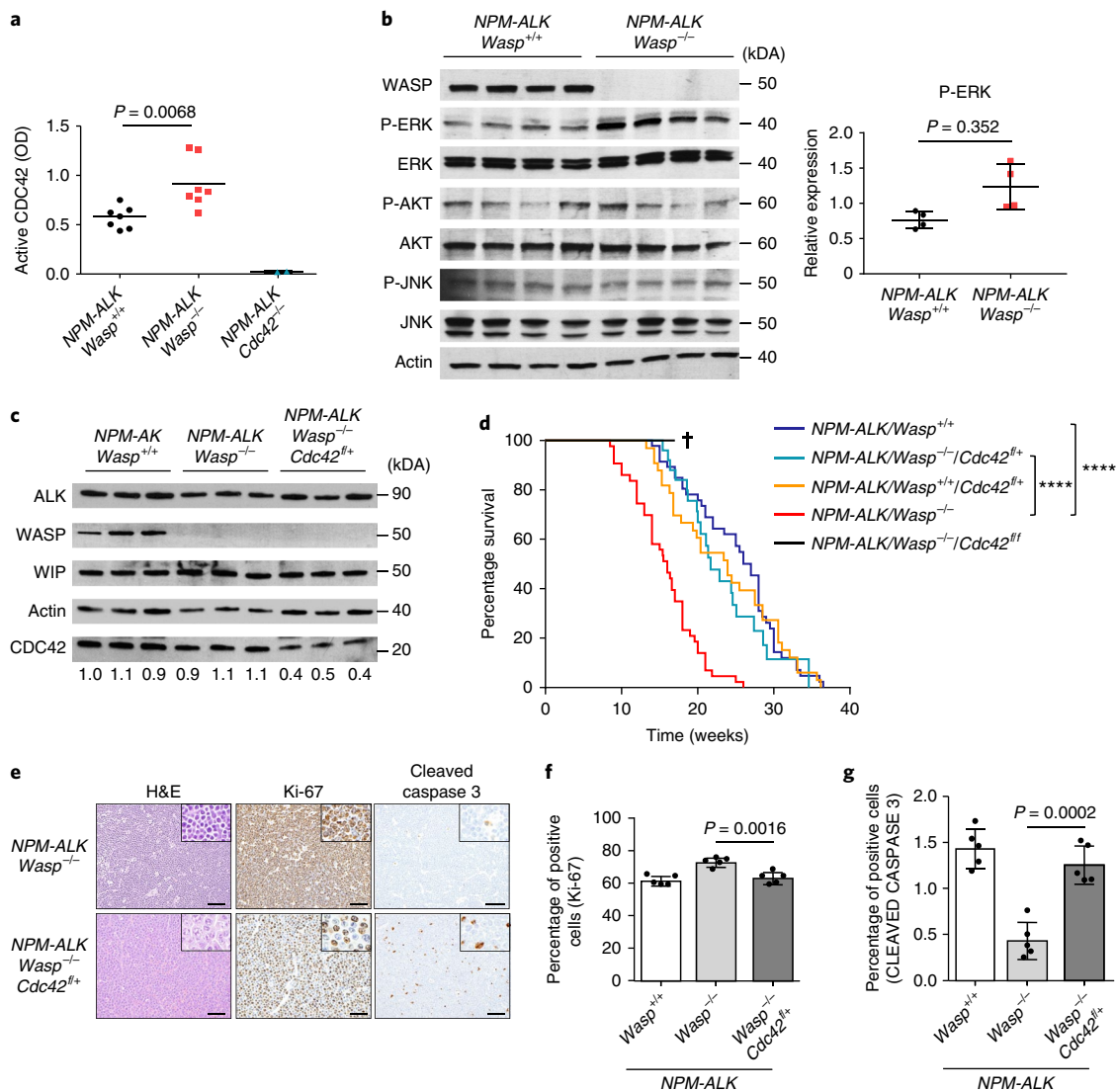


**Fig. 3 | CDC42 and ERK hyperactivation in WASP-deficient lymphoma. a**, Quantification of active GTP-bound CDC42 using CDC42 G-LISA assay kit on cell lines derived from *NPM-ALK* lymphoma with the indicated genotypes (*NPM-ALK/Wasp*<sup>+/+</sup> and *NPM-ALK/Wasp*<sup>-/-</sup>, *n* = 7). *Cdc42* knockout cell lines (*NPM-ALK/Cdc42*<sup>fl/fl</sup>/*CD4-Cre* cell lines, *n* = 2) were used as a control for the assay. Data are shown as means. Significance was determined by an unpaired, two-tailed Student's *t*-test. **b**, Western blot performed with the indicated antibodies on lymphoma cell lines obtained from *NPM-ALK* transgenic mice with the indicated genotypes (left); quantification of phosphorylated ERK (P-ERK) in lymphoma cell lines (right) (*n* = 4 biologically independent samples). Data are shown as means  $\pm$  s.d.; significance was determined by an unpaired, two-tailed Student's *t*-test. Actin was used as a loading control. Uncropped blots are available in Supplementary Fig. 11. **c**, Western blot analysis for WASP, WIP and CDC42 expression on the indicated lymphoma cell lines. Densitometric values of the CDC42 bands normalized to actin are indicated. The blot is representative of at least two independent experiments with similar results. Actin was used as a loading control. Uncropped blots are available in Supplementary Fig. 11. **d**, Kaplan-Meier survival curves of *NPM-ALK* transgenic mice crossed with *Wasp*<sup>+/+</sup> or *Wasp*<sup>-/-</sup> mice with *Cdc42* haploinsufficiency (blue, *NPM-ALK/Wasp*<sup>+/+</sup>, *n* = 35 mice; light blue, *NPM-ALK/Wasp*<sup>-/-</sup>/*Cdc42*<sup>fl/fl</sup>/*CD4-Cre*, *n* = 24; red, *NPM-ALK/Wasp*<sup>-/-</sup>, *n* = 30; black, *NPM-ALK/Wasp*<sup>-/-</sup>/*Cdc42*<sup>fl/fl</sup>/*CD4-Cre*, *n* = 8; orange, *NPM-ALK/Wasp*<sup>+/+</sup>/*Cdc42*<sup>fl/fl</sup>/*CD4-Cre*, *n* = 34). The number of mice for each genotype is indicated. \*\*\*\**P* < 0.0001; significance was determined by log-rank (Mantel-Cox) test. **e**, Representative H&E stain (left) and immunohistochemistry for Ki-67 (middle) and cleaved caspase 3 (right), performed on *NPM-ALK* lymphoma with the indicated genotypes (*n* = 4 mice for each genotype). Scale bar, 100  $\mu$ m. Insets: high-magnification images. **f, g**, Quantification of Ki-67 (**f**) and cleaved caspase 3 (**g**) positive cells in *NPM-ALK* lymphoma with the indicated genotypes (*n* = 5 mice for each genotype). Data are shown as means  $\pm$  s.d.; significance was determined by an unpaired, two-tailed Student's *t*-test.

by ALK activity. Knocking-down *ALK* expression with an inducible shRNA system<sup>32</sup>, led to increased *WASP* and *WIP* mRNA and protein expression (Fig. 5c,d). Consistently, inhibition of ALK activity by the ALK inhibitors crizotinib and alectinib resulted in increased *WASP* and *WIP* mRNA expression (Fig. 5e). Conversely, doxycycline-inducible expression of oncogenic ALK in ALK-negative lymphoma cells down-regulated the expression of both *WASP* and *WIP* (Supplementary Fig. 5b). Treatment of cells with azacitidine, which

is known to restore expression of genes, such as *LAT* and *ZAP70*, that are repressed by ALK through methylation<sup>30,31</sup>, did not change *WASP* and *WIP* expression (Supplementary Fig. 5c,d). Oncogenic ALK activates several downstream pathways, with *STAT3* and *C/EBP- $\beta$*  representing key downstream effectors<sup>16</sup>. Knock-down of either *STAT3* or *C/EBP- $\beta$*  resulted in an increased *WASP* and *WIP* mRNA and protein levels (Fig. 5f and Supplementary Fig. 5e-g). Taken together, these data indicate that ALK oncogenic activity

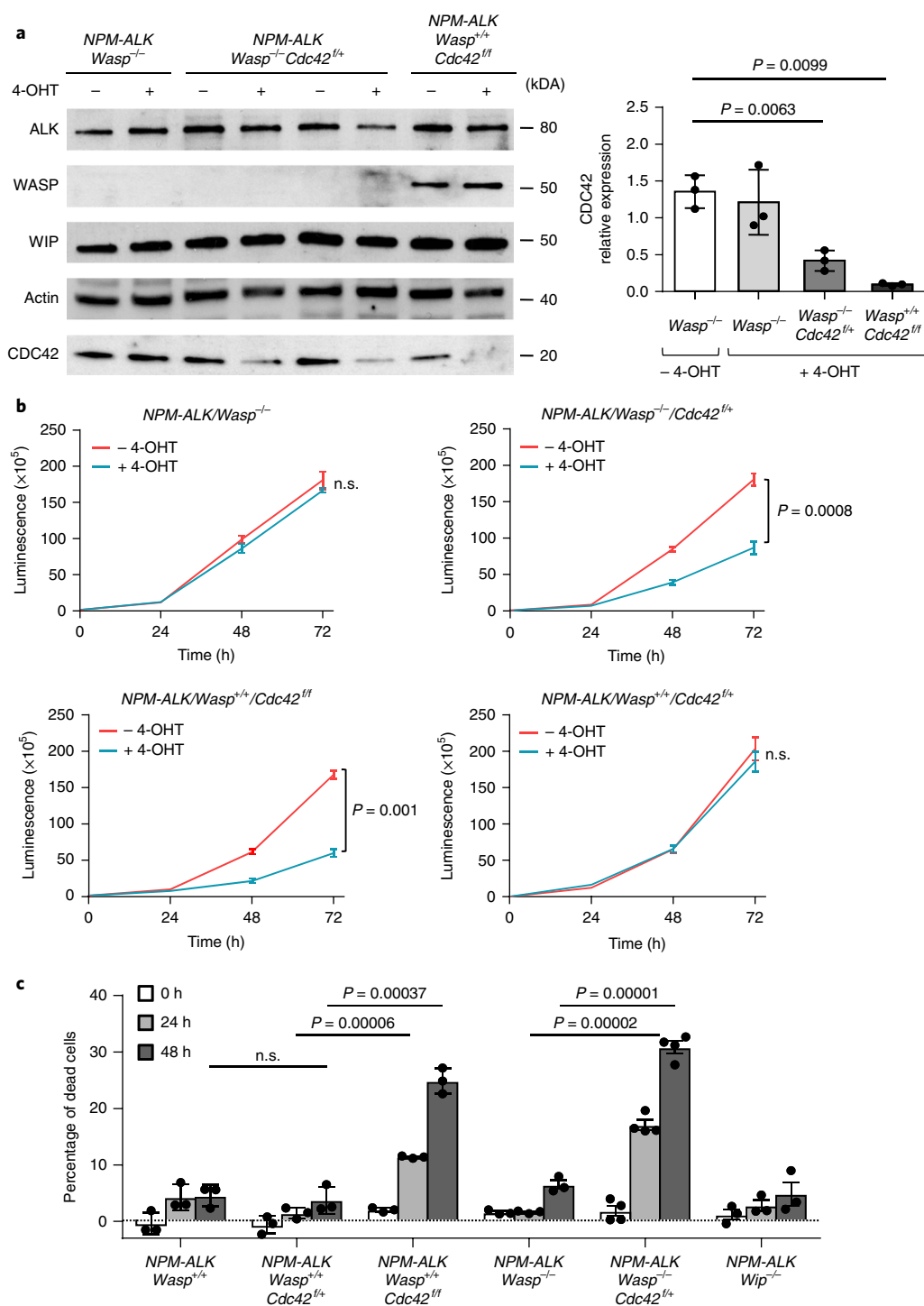


**Fig. 4 | CDC42 is essential for the survival of WASP-deficient lymphoma cells. a**, Western blot analysis for ALK, WASP, WIP and CDC42 on lymphoma cell lines obtained from *NPM-ALK* transgenic mice with the indicated genotypes, transduced with *Cre<sup>ERT2</sup>* and treated with 10 nM 4-hydroxytamoxifen (4-OHT) for 4 h (left). The blot is representative of three independent experiments with similar results. Actin was used as a loading control. Uncropped blots are available in Supplementary Fig. 11. Mean protein expression of CDC42 in mouse cell lines that were treated with 4-OHT or were not treated (right). Data are shown as means  $\pm$  s.d. from three independent experiments with similar results; significance was determined by an unpaired, two-tailed Student's *t*-test. **b**, Cell growth assay performed on lymphoma cell lines obtained from *NPM-ALK* transgenic mice with the indicated genotypes, transduced with *Cre<sup>ERT2</sup>* and treated with 4-OHT. Measurements were taken at the indicated time points ( $n = 3$  biologically independent samples). Data are shown as means  $\pm$  s.e.m.; significance was determined by unpaired, two-tailed Student's *t*-test; n.s., not significant. **c**, Apoptosis analysis performed on lymphoma cell lines obtained from *NPM-ALK* transgenic mice with the indicated genotypes that were treated as in **a**. Measurements were taken at the indicated time points by TMRM staining and flow cytometry analysis. The percentage of dead cells was calculated above background ( $n = 3$  independent experiments). Data are shown as means  $\pm$  s.d.; significance was determined by unpaired, two-tailed Student's *t*-test.

impairs WASP and WIP expression by a transcriptional repression mediated by STAT3 and C/EBP- $\beta$ . To investigate if STAT3 and C/EBP- $\beta$  might directly regulate expression of *WAS* and *WIPF1* genes, we performed chromatin immunoprecipitation and sequencing (ChIP-seq) on ALCL cell lines treated with crizotinib. As expected, 3h of treatment with crizotinib blocked ALK phosphorylation that in turn resulted in a marked de-phosphorylation of STAT3 without affecting total STAT3 levels (Supplementary Fig. 6a). When ALK was active, STAT3 bound genome-wide, whereas in the presence of crizotinib STAT3 binding was almost completely abrogated throughout the genome (Fig. 5g and Supplementary Fig. 6c), including at loci proximal to both the *WAS* and *WIPF1* genes (Fig. 5h,i). In contrast, C/EBP- $\beta$  bound to *WAS* and *WIPF1* genes but its binding was not affected by ALK blockade (Fig. 5h,i and Supplementary Fig. 6b,c). Remarkably, STAT3 and C/EBP- $\beta$  binding sites co-localized with H3K4me3 and H3K27Ac marks indicating that they could functionally contribute to WASP and WIP expression (Supplementary Fig. 6d). Thus, our results are consistent with a model by which STAT3 and C/EBP- $\beta$  regulate WASP and WIP expression where STAT3 regulation directly depends on an ALK-mediated activation.

**WASP and WIP abundance control lymphoma growth.** As absence of WASP accelerates lymphoma growth in mouse models, we reasoned that decreased WASP and WIP expression could contribute also to the biology of human ALK+ ALCL. To test this hypothesis, we forcibly re-expressed WASP and WIP in ALCL cells by using a doxycycline-inducible lentiviral vector. Transduction with WASP vector alone did not increase WASP expression (data not shown), whereas transduction with WIP lentivirus induced a moderate increase in endogenous WASP (Supplementary Fig. 7a), confirming that the levels of WASP in ALCL are regulated by WIP as they are in normal T cells. When ALCL cells were co-transduced with both WASP and WIP lentiviruses, WASP expression was comparable to normal T cells (Fig. 6a). On WASP and WIP induction, the GTP-bound form of CDC42 markedly decreased in ALCL cells, thus confirming that the WASP expression level regulates the abundance of active CDC42 also in human ALCL cell lines (Fig. 6b). Next, we found that ALCL cell lines with induced WASP and WIP expression had impaired growth in vitro (Supplementary Fig. 7b–d) associated with an increased fraction of cells arrested in G1 phase of the cell cycle (Supplementary Fig. 7e). Consistently, the growth of ALCL mouse xenografts was significantly reduced when WASP and WIP expression was induced in vivo (Fig. 6c). Induced expression of WASP in ALCL xenografts was associated with a significant

increase in apoptosis and a decrease in proliferation (Fig. 6d,e and Supplementary Fig. 7f). Furthermore, the activation of the MAPK pathway, as measured by phosphorylated ERK1/2 levels, decreased upon WASP and WIP induction, concomitant with an increase in cleaved caspase 3 (Supplementary Fig. 4b). Thus, the low expression of WASP and WIP contributes the pathogenesis of ALCL, and the restoration of their expression impairs lymphoma growth by decreasing the amount of active CDC42 and MAPK signaling.

**MAPK activation is a therapeutic vulnerability in WASP-deficient lymphoma.** Finally, we reasoned that increased MAPK signaling in ALCL cells expressing low levels of WASP could represent a therapeutic vulnerability. To test this concept, we treated lymphoma cells with trametinib, a MEK inhibitor approved for melanoma treatment and currently in trial for lymphoma (NCT00687622). Lymphomas from *NPM-ALK/Wasp<sup>-/-</sup>* mice were more sensitive than wild-type lymphoma to trametinib (Fig. 6f) as well as to additional MEK inhibitors (selumetinib, MEK162 and PD0325901) (Supplementary Fig. 8a). Consistently, human ALCL with low WASP expression (SU-DHL1 and JB6) were also more sensitive than ALCL with higher WASP expression (TS and L82) (Supplementary Fig. 8b). Considering that ALK inhibitors have potent clinical activity in ALK+ ALCL<sup>16,33</sup>, we also investigated whether MEK inhibition could potentiate ALK inhibitors in a combination therapy, as has been recently suggested for ALK-rearranged lung cancer<sup>34</sup>. In vitro, *NPM-ALK* lymphoma lines were sensitive to crizotinib, and the combination with trametinib further potentiated crizotinib activity (Supplementary Fig. 8c). In vivo, trametinib alone did not have an effect against *NPM-ALK* lymphoma, as expected from similar experiment in ALK+ lung cancer<sup>34</sup>. In contrast, the combination of trametinib with crizotinib was more potent than crizotinib alone for the treatment of *NPM-ALK/Wasp<sup>-/-</sup>* but not wild-type lymphoma (Fig. 6g), supporting the concept that the MAPK pathway is a therapeutic vulnerability in WASP-deficient lymphoma.

**Lymphocytes from patients with WAS show increased CDC42 activity and MAPK signaling.** Patients with WAS have a variety of mutations in the *WAS* gene that result in a variably reduced abundance or function of WASP<sup>7</sup>. As in human ALCL and mouse models, the reduced or absent expression of WASP increases the abundance of active CDC42, and so we reasoned that lymphocytes from patients with absent or very low WASP expression should display higher CDC42 activation than control lymphocytes. We characterized Epstein–Barr virus (EBV)-immortalized B lymphocytes from three patients with WAS with defined *WAS* mutations (Supplementary

**Fig. 5 | Oncogenic ALK down-regulates WASP and WIP expression through STAT3 and C/EBP $\beta$ .** **a**, Western blot performed on human ALK+ ALCL cell lines and ALK- T lymphoma lines or normal T cells blotted with the indicated antibodies. The blot is representative of two independent experiments with similar results. Actin was used as a loading control. Uncropped blots are available in Supplementary Fig. 11. **b**, Quantitative real-time PCR (qRT-PCR) expression analysis of *WASP* and *WIP* mRNA in human ALK+ ALCL cell lines and ALK- T lymphoma lines or normal T cells ( $n=3$  independent experiments). Data are shown as means  $\pm$  s.d. **c**, qRT-PCR expression analysis of *WASP* and *WIP* mRNA on two representative ALK+ ALCL human cell lines (TS and SU-DHL1) transduced with a doxycycline-dependent ALK shRNA or control shRNA ( $n=3$  independent experiments). Data are shown as means  $\pm$  s.d.; significance was determined by an unpaired, two-tailed Student's *t*-test. **d**, Western blot analysis on the same cells as in **c** collected at 96 h. Densitometric values of the bands are indicated. One representative experiment out of three performed is shown. Actin was used as a loading control. Uncropped blots are available in Supplementary Fig. 11. **e**, qRT-PCR expression analysis of *WASP* and *WIP* mRNA on three representative ALK+ ALCL human cell lines (TS, JB6 and Karpas-299) treated with two different ALK inhibitors, alectinib (30 nM) and crizotinib (100 nM) for 12 h (JB6 and Karpas-299) or 24 h (TS) ( $n=3$  independent experiments). Data are shown as means  $\pm$  s.d.; significance was determined by an unpaired, two-tailed Student's *t*-test. **f**, qRT-PCR expression analysis of *WASP* and *WIP* mRNA on the ALK+ TS cell line in which the expression of STAT3 has been knocked down by the specific shRNA. The corresponding western blot of the shRNA knockdown is shown on the left. Two independent shRNA have been used for each knockdown assay (indicated with numbers 1 and 2). A scrambled shRNA has been used as control ( $n=3$  independent experiments). Data are shown as means  $\pm$  s.d.; significance was determined by an unpaired, two-tailed Student's *t*-test. The blot is representative of three independent experiments with similar results. Actin was used as a loading control. Uncropped blots are available in Supplementary Fig. 11. **g**, Heatmaps (left) and metaplots (right) of global STAT3 peaks obtained by ChIP-seq in SU-DHL1 cells treated for 3h with crizotinib (300 nM). **h,i**, STAT3 or C/EBP- $\beta$  ChIP-seq tracks at *WAS* (**h**) and *WIPF1* (**i**) genes on two representative ALK+ ALCL human cell lines (JB6 and SU-DHL1) treated for 3h with crizotinib (300 nM). The experiment was performed once on two independent cell lines with similar results.

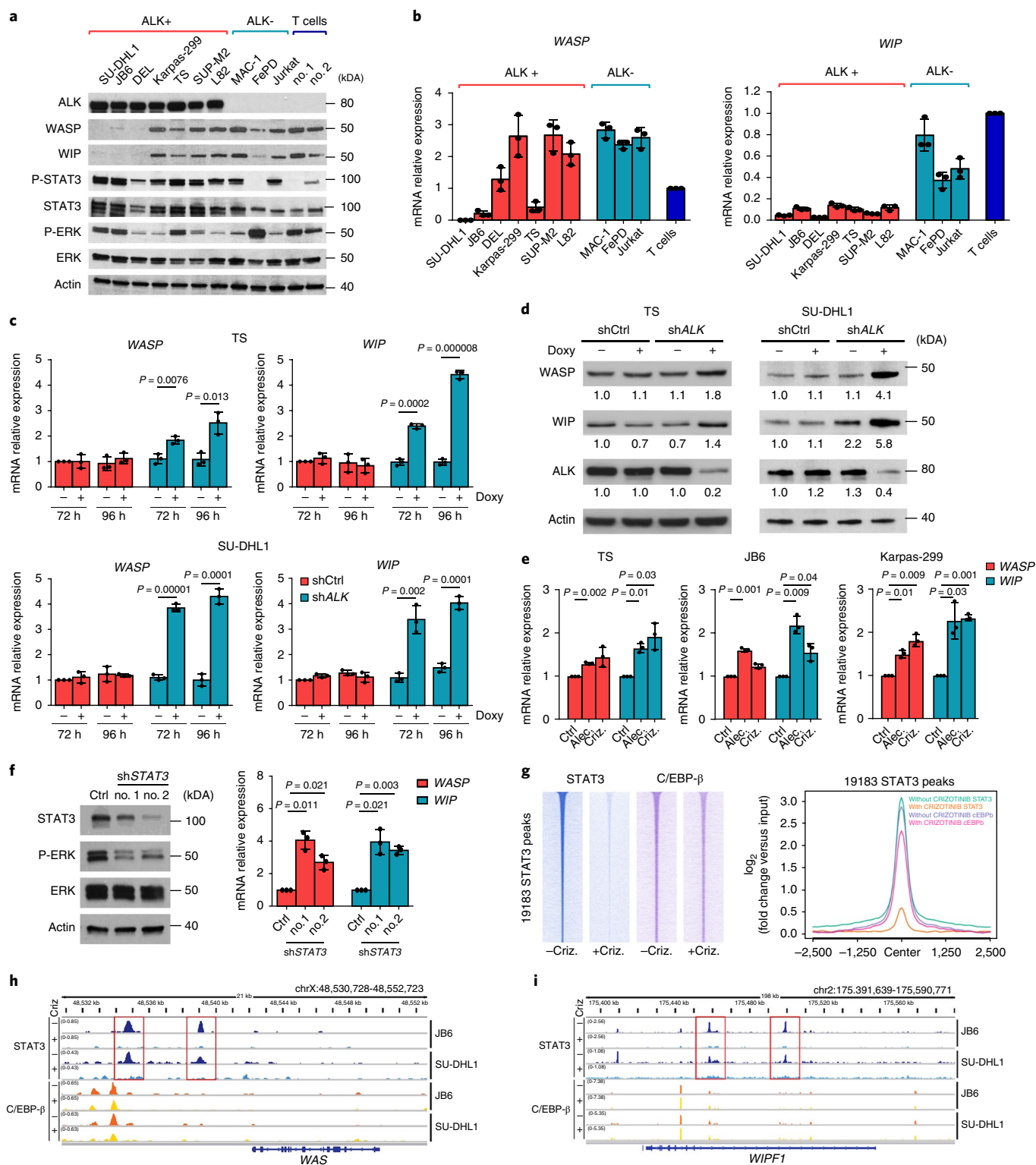


Fig. 9a) and low or absent WASP expression (Supplementary Fig. 9b). Indeed, lymphocytes from patients with WAS showed higher levels of CDC42 activation than control cells (Supplementary Fig. 9c), in keeping with observations in *NPM-ALK* lymphoma cells. In addition, WAS lymphocytes showed decreased phosphorylation of STAT3 and AKT, consistent with defective cytokine production in WASP-deficient lymphocytes<sup>35</sup>, but they showed higher levels of ERK and S6 phosphorylation, consistent with increased activation of the MAPK pathway (Supplementary Fig. 9b). These

data show that lymphocytes from patients with WAS with absent WASP expression have higher activity of CDC42 and MAPK signaling, suggesting the possibility that the predisposition of patients with WAS to lymphoma could be associated to an intrinsic aberrant signaling in their lymphocytes.

**Discussion**

WASP and WIP are essential regulators of the cytoskeleton in hematopoietic cells. Proper cytoskeletal regulation is fundamental for a



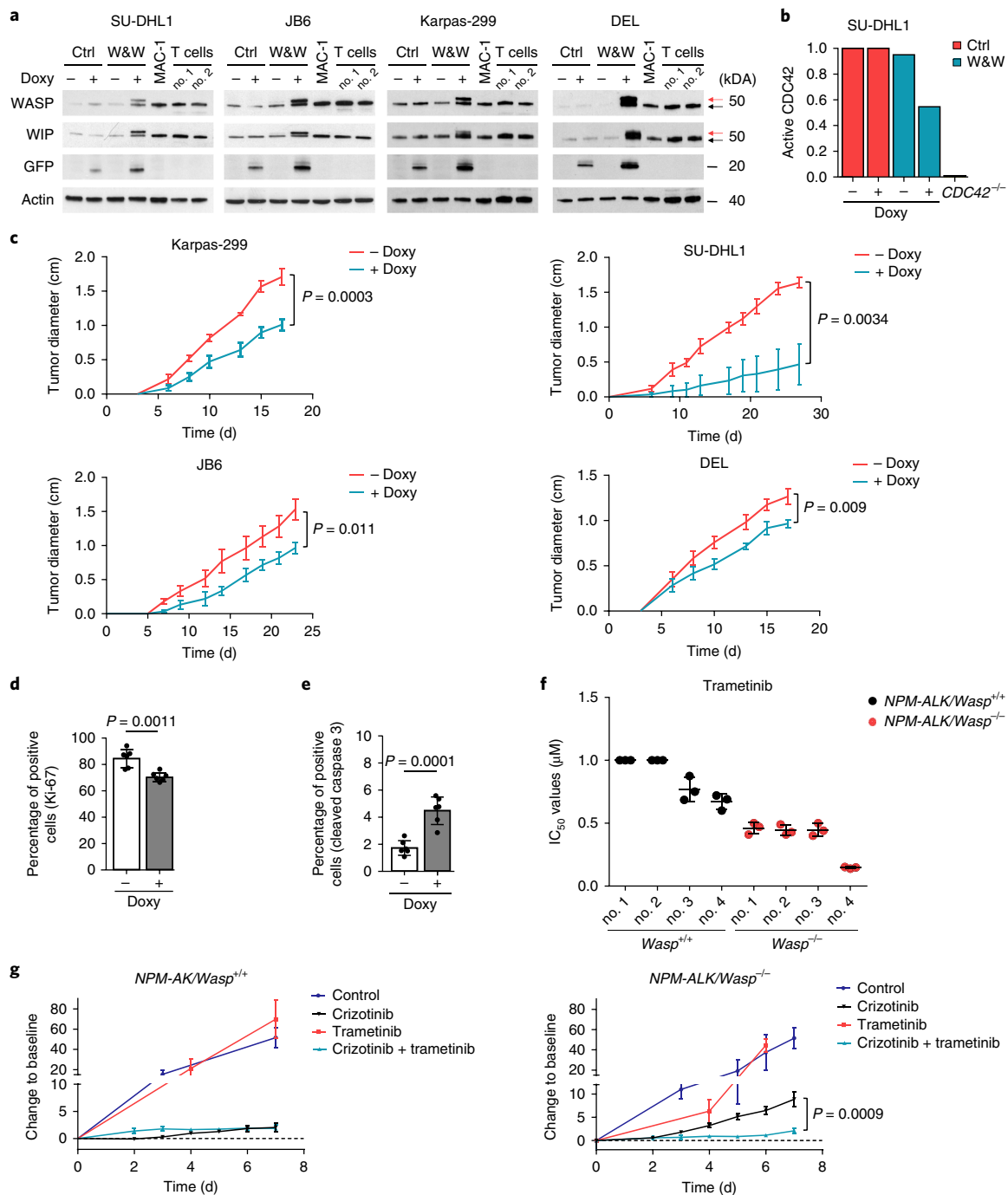


**Fig. 6 | MAPK pathway is a therapeutic vulnerability in WASP-deficient cells. a**, Western blot analysis of ALK+ ALCL cell lines (SU-DHL1, JB6, Karpas-299 and DEL) transduced with doxycycline (doxy)-inducible lentivirus co-expressing WASP and WIP (W&W) or a control reporter GFP (Ctrl). Black arrows: endogenous WASP and WIP; red arrows: Flag-tagged WASP and WIP. The MAC-1 cell line and normal T cells were used as controls. The blot is representative of at least two independent experiments with similar results. Actin was used as a loading control. Uncropped blots are available in Supplementary Fig. 11. **b**, Quantification of active GTP-bound CDC42 on the SU-DHL1 cell line after induction of WASP and WIP expression using CDC42 activation assay kit. CDC42 knockout (*CDC42*<sup>-/-</sup>) cells were used as a negative control of the assay. One representative of two independent experiments in triplicates is shown. **c**, Growth of xenografted tumors in Nod scid gamma (NSG) mice injected with ALK+ ALCL cells (Karpas-299, SU-DHL1, JB6 and DEL) transduced with doxycycline-inducible WASP and WIP vectors. Mice were treated with normal (red line) or doxycycline-treated (light blue line) water ( $n = 6$  independent tumors). Data are shown as means  $\pm$  s.e.m.; significance was determined by an unpaired, two-tailed Student's *t*-test. Doxycycline treatment started at day 0 when cells were injected sub cutis. **d, e**, Quantification of Ki-67 (**d**) and cleaved Caspase 3 (**e**) positive cells in ALK+ ALCL xenograft lymphoma as in **c** ( $n = 6$  tumors). Data are shown as means  $\pm$  s.e.m.; significance was determined by an unpaired, two-tailed Student's *t*-test. **f**, Sensitivity to trametinib of mouse *NPM-ALK* lymphoma cells with the indicated genotypes treated for 72 h with trametinib. Shown are absolute half-maximal inhibitory concentration ( $IC_{50}$ ) values ( $\mu$ M,  $n = 3$  biologically independent samples). Data are shown as means  $\pm$  s.d. **g**, Growth of WASP wild type or knockout *NPM-ALK* lymphoma cells grafted in NSG mice treated with trametinib alone ( $1.5 \text{ mg kg}^{-1}$ ) or crizotinib ( $30 \text{ mg kg}^{-1}$ ) alone or in combination with trametinib ( $1.5 \text{ mg kg}^{-1}$ ). Values shown are the changes in tumor volume from baseline ( $n = 5$  independent tumors). Data are shown as means  $\pm$  s.e.m.; significance was determined by an unpaired, two-tailed Student's *t*-test.

variety of functions in lymphocytes and other hematopoietic cells, including lymphocyte proliferation and homeostasis<sup>7</sup>. Patients with WAS have a variable degree of immunodeficiency and an overall increased risk of developing hematologic malignancies, mostly lymphomas, that are thought to develop because of the immunodeficiency state<sup>10</sup>. In this work, we provide evidence that WASP is an oncosuppressor in T lymphocytes, and we identify ALCL as a specific subtype of T cell lymphoma in which WASP and WIP expression is selectively downregulated and contributes to lymphoma pathogenesis. An interesting expansion of this work would be to study WASP and WIP expression in B cell lymphoma or other hematologic malignancies. Furthermore, we provide evidence that the levels of the Rho GTPase CDC42 are essential for the tumor-suppressor functions of WASP. The acceleration of lymphoma development in *Wasp*<sup>-/-</sup> mice was dependent on the abundance of CDC42 in lymphoma cells; *Wasp*<sup>-/-</sup> lymphomas had significantly higher amount of active GTP-bound CDC42 and a reduction of about half CDC42 protein was sufficient to revert the phenotype in vitro and in vivo (Fig. 3d and Fig. 4b,c). Similar WASP-dependent regulation of active CDC42 was found in human ALCL (Fig. 6b) as well as in immortalized B lymphocytes from patients with WAS (Supplementary Fig. 9c), demonstrating that active CDC42 accumulates in normal and tumor lymphocytes in the absence of WASP.

Considering the known role of WASP and WIP in T cell activation, we evaluated the possibility that the accelerated lymphoma development observed in WASP- and WIP-deficient mice could be associated to a defective immunosurveillance. However, several findings suggest that defective immunosurveillance is not sufficient to explain the accelerated lymphomagenesis in WASP- and WIP-deficient mice. First, in contrast to other classical immunodeficient strains such as Nod scid mice, *Wasp*<sup>-/-</sup> and *Wip*<sup>-/-</sup> mice do not develop spontaneous lymphomas or other tumors<sup>2,9</sup>, thus implying that the level of immunodeficiency is probably mild in these mice. Second, T cell functional defects are more pronounced in *Wip*<sup>-/-</sup> mice than in *Wasp*<sup>-/-</sup> mice<sup>2</sup>, yet the acceleration of lymphomagenesis is comparable in the two genetic backgrounds. Third, *Wasp*<sup>-/-</sup>/*Cdc42*<sup>2/+</sup>/*CD4-Cre* T cells had defective T cell proliferation (Supplementary Fig. 10a) and defective MAPK pathway activation (Supplementary Fig. 10b) similar to *Wasp*<sup>-/-</sup> T cells, yet the loss of one copy of *Cdc42* is sufficient to revert the lymphoma acceleration observed in *Wasp*<sup>-/-</sup> mice (Fig. 3d). Fourth, if the immunodeficiency of *Wasp*<sup>-/-</sup> mice would be a major contribution to the accelerated lymphomagenesis, *Wasp*<sup>-/-</sup> lymphoma should have incurred into a limited immunoeediting and have growth significantly impaired when transplanted into immunocompetent mice. In contrast, wild-type and *Wasp*<sup>-/-</sup> lymphoma grew equally in immunocompetent mice (Supplementary Fig. 10c). Finally, experiments in human ALCL clearly show that the cellular levels of WASP and WIP intrinsically contribute to lymphoma growth in vitro and in vivo.

We showed that WASP and WIP expression are selectively decreased in ALCL, a subtype of T cell lymphoma that can be driven by translocations involving the *ALK* gene in ALK+ ALCL or by translocations involving other tyrosine kinases or phosphatases in ALK- ALCL<sup>14,15</sup>. Interestingly, aberrant STAT3 activation is frequent in both ALK+ and ALK- ALCL where STAT3 phosphorylation is directly controlled by ALK or other oncogenic tyrosine kinases, such as ROS1 and TYK2<sup>14,36</sup>. We showed that ALK oncogenic activity mediates downregulation of WASP and WIP through a STAT3 and C/EBP- $\beta$  dependent transcriptional repression. ChIP-seq experiments showed that abrogation of STAT3 activation by ALK inhibitors resulted in a profound genome-wide loss of STAT3 binding as well as that at *WAS* and *WIPF1* genes (Fig. 5g-i and Supplementary Fig. 6b,c). Therefore, WASP and WIP downregulation could represent a common feature of T cell lymphomas where the activity of STAT3 predominates, typically those induced by deregulated tyrosine kinases such as ALCL. In contrast, AITL

and PTCL are more dependent on a tonic TCR signaling that relies on the maintenance of cytoskeletal signaling functions in which WASP and WIP are essential. However, TCR ligation induces WASP degradation that in turn modifies assembly of F-actin. Thus, reduced levels of WASP after TCR engagement could also play a role in downstream signaling in normal T cells<sup>37</sup>.

Other mechanisms may contribute to the downregulation of WASP or WIP in ALCL. For example, a recent study showed that NPM-ALK directly phosphorylates Tyr102 of WASP; this phosphorylation impairs the binding of WASP to WIP and increases proteasome-dependent WASP degradation<sup>38</sup>, overall confirming that ALK downregulates WASP expression by multiple mechanisms. In contrast to our findings, however, this study concluded that WASP contributes to the oncogenic activity of ALK. This discrepancy probably originates from a different approach that focused on abrogating the residual WASP expression by shRNA rather than investigating the overall low levels of WASP in ALCL.

Whereas *WAS* and *WIPF1* mutations in ALCL have not been systematically studied, interestingly somatic loss of function (*WAS*<sup>G229E</sup>) or frame-shift mutations (*WAS*<sup>G333fs</sup> and *WAS*<sup>P329fs</sup>) leading to premature WASP truncation similar to patients with WAS have been detected in 4.6% of PTCL-NOS<sup>19</sup>, raising the intriguing possibility that a fraction of other T cell lymphomas rely on somatic inactivation of WASP. In an ongoing effort to characterize *WAS* and *WIPF1* genes in ALCL, we performed whole-exome sequencing in six cases of ALK+ ALCL. No somatic mutations of the *WAS*, *WIPF1* and *CDC42* genes were found, but deletions of chromosome X in the region containing the *WAS* gene was detected in two out of six cases, suggesting that gene deletion could be an additional mechanism for WASP inactivation in ALCL. Furthermore, we found one case with a mutation of the intersectin 2 (*ITSN2*) gene and two cases with mutations of the Myosin Heavy Chain 8 (*MYH8*) genes (Supplementary Table 1). *ITSN2* is a GEF for CDC42 and regulates its activation<sup>39</sup> and interacts directly with WASP<sup>40</sup>. *MYH8* is associated with the PAK and GTPase pathways. Interestingly, this gene was recently found also mutated in ALK- ALCL<sup>14</sup>. These are limited observations that need to be expanded in larger series of cases but could underlie additional potential mechanisms that alter the CDC42-WASP axis in T cell lymphoma.

Taken together, it is tempting to propose that T cell lymphomas can be divided into two main categories. In T cell lymphomas that retain TCR signaling dependence, such as PTCL-NOS and AITL, WASP and WIP functions are maintained, at least initially, as they are key molecules for the immunological synapse and TCR signaling; once a lymphoma is established, inactivating mutations of WASP could be further selected by providing additional growth advantage. On the other hand, in T cell lymphomas that lost TCR signaling and depend on aberrant tyrosine kinase activity, such as ALCL, WASP and WIP are lost or downregulated as they act as tumor suppressors; their downregulation provides a biological advantage by increased active CDC42 and MAPK signaling. In these lymphomas, the hyper-activated MAPK pathway could represent an actionable therapeutic vulnerability when combined with the inhibition of ALK, which is the driver oncogene in ALK+ ALCL. Thus, inhibition of both ALK and MEK inhibitors could represent a more powerful therapeutic strategy in ALK+ ALCL, possibly for those patients who respond poorly to crizotinib<sup>33</sup>. A similar concept has been recently suggested for ALK+ lung cancers<sup>34</sup>.

In conclusion, by combining genetic and functional assays we have demonstrated an unexpected role for WASP and WIP as oncosuppressor proteins in lymphomas. Mechanistically, we have shown that the levels of CDC42 activation are increased in the absence of a binding to WASP, leading to increased proliferation and survival of lymphoma cells. The activation of CDC42 and MAPK pathway provides a therapeutic vulnerability in lymphoma with low WASP expression.

## Online content

Any methods, additional references, Nature Research reporting summaries, source data, statements of data availability and associated accession codes are available at <https://doi.org/10.1038/s41591-018-0262-9>.

Received: 3 December 2017; Accepted: 25 September 2018;  
Published online: 3 December 2018

## References

- Sullivan, K. E., Mullen, C. A., Blaese, R. M. & Winkelstein, J. A. A multiinstitutional survey of the Wiskott–Aldrich syndrome. *J. Pediatr.* **125**, 876–885 (1994).
- Anton, I. M. et al. WIP deficiency reveals a differential role for WIP and the actin cytoskeleton in T and B cell activation. *Immunity* **16**, 193–204 (2002).
- de la Fuente, M. A. et al. WIP is a chaperone for Wiskott–Aldrich syndrome protein (WASP). *Proc. Natl Acad. Sci. USA* **104**, 926–931 (2007).
- Ramesh, N. & Geha, R. Recent advances in the biology of WASP and WIP. *Immunol. Res.* **44**, 99–111 (2009).
- Ramesh, N., Anton, I. M., Hartwig, J. H. & Geha, R. S. WIP, a protein associated with wiskott-aldrich syndrome protein, induces actin polymerization and redistribution in lymphoid cells. *Proc. Natl Acad. Sci. USA* **94**, 14671–14676 (1997).
- Abdul-Manan, N. et al. Structure of Cdc42 in complex with the GTPase-binding domain of the ‘Wiskott–Aldrich syndrome’ protein. *Nature* **399**, 379–383 (1999).
- Thrasher, A. J. & Burns, S. O. WASP: a key immunological multitasker. *Nat. Rev. Immunol.* **10**, 182–192 (2010).
- Massaad, M. J., Ramesh, N. & Geha, R. S. Wiskott–Aldrich syndrome: a comprehensive review. *Ann. N. Y. Acad. Sci.* **1285**, 26–43 (2013).
- Snapper, S. B. et al. Wiskott–Aldrich syndrome protein-deficient mice reveal a role for WASP in T but not B cell activation. *Immunity* **9**, 81–91 (1998).
- Ochs, H. D. & Thrasher, A. J. The Wiskott–Aldrich syndrome. *J. Allergy Clin. Immunol.* **117**, 725–738 (2006). quiz 739.
- Recher, M. et al. B cell-intrinsic deficiency of the Wiskott–Aldrich syndrome protein (WASP) causes severe abnormalities of the peripheral B-cell compartment in mice. *Blood* **119**, 2819–2828 (2012).
- Boddicker, R. L., Razidlo, G. L. & Feldman, A. L. Genetic alterations affecting GTPases and T-cell receptor signaling in peripheral T-cell lymphomas. *Small GTPases* **29**, 1–7 (2016).
- Scarfo, I. et al. Identification of a new subclass of ALK-negative ALCL expressing aberrant levels of ERBB4 transcripts. *Blood* **127**, 221–232 (2016).
- Crescenzo, R. et al. Convergent mutations and kinase fusions lead to oncogenic STAT3 activation in anaplastic large cell lymphoma. *Cancer Cell* **27**, 516–532 (2015).
- Parrilla Castellar, E. R. et al. ALK-negative anaplastic large cell lymphoma is a genetically heterogeneous disease with widely disparate clinical outcomes. *Blood* **124**, 1473–1480 (2014).
- Werner, M. T., Zhao, C., Zhang, Q. & Wasik, M. A. Nucleophosmin-anaplastic lymphoma kinase: the ultimate oncogene and therapeutic target. *Blood* **129**, 823–831 (2017).
- Yoo, H. Y. et al. A recurrent inactivating mutation in RHOA GTPase in angioimmunoblastic T cell lymphoma. *Nat. Genet.* **46**, 371–375 (2014).
- Sakata-Yanagimoto, M. et al. Somatic RHOA mutation in angioimmunoblastic T cell lymphoma. *Nat. Genet.* **46**, 171–175 (2014).
- Palomero, T. et al. Recurrent mutations in epigenetic regulators, RHOA and FYN kinase in peripheral T cell lymphomas. *Nat. Genet.* **46**, 166–170 (2014).
- Abate, F. et al. Activating mutations and translocations in the guanine exchange factor VAV1 in peripheral T-cell lymphomas. *Proc. Natl Acad. Sci. USA* **114**, 764–769 (2017).
- Ambrogio, C. et al. The anaplastic lymphoma kinase controls cell shape and growth of anaplastic large cell lymphoma through Cdc42 activation. *Cancer Res.* **68**, 8899–8907 (2008).
- Colomba, A. et al. Activation of Rac1 and the exchange factor Vav3 are involved in NPM-ALK signaling in anaplastic large cell lymphomas. *Oncogene* **27**, 2728–2736 (2008).
- Choudhari, R. et al. Redundant and nonredundant roles for Cdc42 and Rac1 in lymphomas developed in NPM-ALK transgenic mice. *Blood* **127**, 1297–1306 (2016).
- Swerdlow, S. H. et al. The 2016 revision of the World Health Organization classification of lymphoid neoplasms. *Blood* **127**, 2375–2390 (2016).
- Chiarle, R. et al. NPM-ALK transgenic mice spontaneously develop T-cell lymphomas and plasma cell tumors. *Blood* **101**, 1919–1927 (2003).
- Lanzi, G. et al. A novel primary human immunodeficiency due to deficiency in the WASP-interacting protein WIP. *J. Exp. Med.* **209**, 29–34 (2012).
- Al-Mousa, H. et al. Hematopoietic stem cell transplantation corrects WIP deficiency. *J. Allergy Clin. Immunol.* **139**, 1039–1040 e1034 (2017).
- Notarangelo, L. D., Notarangelo, L. D. & Ochs, H. D. WASP and the phenotypic range associated with deficiency. *Curr. Opin. Allergy. Clin. Immunol.* **5**, 485–490 (2005).
- Hill, C. S., Wynne, J. & Treisman, R. The Rho family GTPases RhoA, Rac1, and CDC42Hs regulate transcriptional activation by SRF. *Cell* **81**, 1159–1170 (1995).
- Ambrogio, C. et al. NPM-ALK oncogenic tyrosine kinase controls T-cell identity by transcriptional regulation and epigenetic silencing in lymphoma cells. *Cancer Res.* **69**, 8611–8619 (2009).
- Hassler, M. R. et al. Insights into the pathogenesis of anaplastic large-cell lymphoma through genome-wide DNA methylation profiling. *Cell Rep.* **17**, 596–608 (2016).
- Piva, R. et al. Ablation of oncogenic ALK is a viable therapeutic approach for anaplastic large-cell lymphomas. *Blood* **107**, 689–697 (2006).
- Gambacorti Passerini, C. et al. Crizotinib in advanced, chemoresistant anaplastic lymphoma kinase-positive lymphoma patients. *J. Natl Cancer. Inst.* **106**, djt378 (2014).
- Hrustanovic, G. et al. RAS-MAPK dependence underlies a rational polytherapy strategy in EML4-ALK-positive lung cancer. *Nat. Med.* **21**, 1038–1047 (2015).
- Rivers, E. & Thrasher, A. J. Wiskott–Aldrich syndrome protein: emerging mechanisms in immunity. *Eur. J. Immunol.* **47**, 1857–1866 (2017).
- Chiarle, R. et al. Stat3 is required for ALK-mediated lymphomagenesis and provides a possible therapeutic target. *Nat. Med.* **11**, 623–629 (2005).
- Watanabe, Y. et al. T-cell receptor ligation causes Wiskott–Aldrich syndrome protein degradation and F-actin assembly downregulation. *J. Allergy Clin. Immunol.* **132**, 648–655 e641 (2013).
- Murga-Zamalloa, C. A. et al. NPM-ALK phosphorylates WASP Y102 and contributes to oncogenesis of anaplastic large cell lymphoma. *Oncogene* **36**, 2085–2094 (2017).
- Zhang, J. et al. Intersectin 2 controls actin cap formation and meiotic division in mouse oocytes through the Cdc42 pathway. *FASEB J* **31**, 4277–4285 (2017).
- McGavin, M. K. et al. The intersectin 2 adaptor links Wiskott Aldrich Syndrome protein (WASP)-mediated actin polymerization to T cell antigen receptor endocytosis. *J. Exp. Med.* **194**, 1777–1787 (2001).

## Acknowledgements

We thank M.S. Scalzo and D. Corino for technical assistance, and B. Castella for providing purified human T cells. The work has been supported by grant no. FP7 ERC-2009-StG (Proposal No. 242965—‘Lunely’) (R.C.) grant no. R01 CA196703-01 (R.C.); AIRC grant no. MFAG (C.A. and M.C.); National Research Foundation of Korea (NRF) fellowship 2016R1A6A3A03006840 (T.-C.C.); Bando Giovani Ricercatori grant no. 2009-GR 1603126 (M.C.); MINECO/FEDER grant no. SAF2015–70368-R and Fundación Ramón Areces (I.M.A.); the Division of Intramural Research, National Institute of Allergy and Infectious Diseases, National Institutes of Health (L.D.N.); and award no. T32GM007753 from the National Institute of General Medical Sciences (S.H.C.) (the content is solely the responsibility of the authors and does not necessarily represent the official views of the National Institute of General Medical Sciences or the National Institutes of Health); and in part by awards from the National Institutes of Health DP2 New Innovator award no. 1DP2CA195762-01 (C.K.); the American Cancer Society Research Scholar award no. RSG-14-051-01-DMC and the Pew-Stewart Scholars in Cancer Research Grant (C.K.); and the European Union Horizon 2020 Marie Skłodowska-Curie Innovative Training Network Grant award no. 675712 for the European Research Initiative for ALK-Related Malignancies (G.G.S., I.M., C.G.P. and R.C.).

## Author contributions

M.M., C.A., T.-C.C., C.P., I.M., S.H.C., M.C., R.D., T.P., E.P., C.M. and C.V. performed experiments. M.M., V.M., C.V. and R. Choudhari performed mice experiments. Q.W. and C.K.C. performed bioinformatics analysis. A.P. analyzed data. R.P. provided gene expression data on lymphoma samples. C.K. provided reagents for ChIP-seq. S.G. and L.G.N. provided WAS patient samples and analyzed data. G.G.S., L.M. and C.G.-P. provided sequencing data on patients with ALCL. A.Z. provided lymphoma cases. I.M.A. contributed mouse strains and analyzed data. C.V. and R. Chiarle conceived and analyzed the experiments. M.M., C.V. and R. Chiarle wrote the manuscript.

## Competing Interests

The authors declare no competing interests.

## Additional information

Supplementary information is available for this paper at <https://doi.org/10.1038/s41591-018-0262-9>.

Reprints and permissions information is available at [www.nature.com/reprints](http://www.nature.com/reprints).

Correspondence and requests for materials should be addressed to C.V. or R.C.

**Publisher's note:** Springer Nature remains neutral with regard to jurisdictional claims in published maps and institutional affiliations.

© This is a U.S. government work and not under copyright protection in the U.S.; foreign copyright protection may apply 2018

## Methods

**Transgenic mice and tumor xenografts.** *CD4-NPM-ALK* transgenic mice<sup>25</sup>, *CD4-Cre*<sup>26</sup>, *Cdc42<sup>fl/fl</sup>*, *Wasp<sup>-/-</sup>* and *Wip<sup>-/-</sup>* (ref. 2) were previously described. *CD4-NPM-ALK*, *Wasp<sup>-/-</sup>* and *Wip<sup>-/-</sup>* mice were bred in C57BL/6 background. NSG immunocompromised mice were purchased from Charles River Laboratories. For subcutaneous xenografts, human ALCL cell lines transduced with inducible lentiviral vectors expressing WASP and WIP complementary DNA were injected in both flanks of NSG mice;  $5 \times 10^6$  cells were resuspended in 150  $\mu$ l PBS and injected. Injected mice were administered drinking water containing doxycycline (1 mg ml<sup>-1</sup>) (Sigma) to express WASP and WIP cDNA. Tumor growth was measured with a caliper every two days. Mice were euthanized at humane endpoint, and tumors were resected with a scalpel and snapped frozen or paraffin fixed in buffer neutral formalin for further experiments.

Mice were treated with trametinib (1.5 mg kg<sup>-1</sup>) or crizotinib (30 mg kg<sup>-1</sup>) or a combination of the two inhibitors by oral gavage once a day for a week. Tumor growth was measured with a caliper every two days. Both drugs were dissolved in 0.5% methylcellulose + 0.05% Tween-80. Mice were euthanized at humane endpoint.

Lymphoma cell lines obtained from *NPM-ALK* transgenic mice were injected subcutaneously in both flanks of syngeneic C57BL/6 or NSG mice, and  $10 \times 10^6$  cells were resuspended in 150  $\mu$ l PBS and injected. Tumor growth was followed as described above.

Mice were handled and treated in accordance with European Community guidelines under the mouse protocol approved by the Italian Ministry of Research (no. 254/2017-PR).

**Cell lines and reagents.** Human ALK+ ALCL cell lines (TS, SU-DHL1, JB6, Karpas-299, DEL, SUP-M2 and L82) and ALK- cell lines (MAC-1, FePD and Jurkat) ALCL cell lines were obtained from DSMZ (German collection of Microorganisms and Cell Cultures). Cell lines were maintained in RPMI 1640 (Lonza) with 10% fetal bovine serum (FBS), 2% penicillin, streptomycin (5 mg ml<sup>-1</sup>), (Gibco) and 1% glutamine (Gibco). Cell lines were grown at 37°C in a humidified atmosphere with 5% CO<sub>2</sub>. ALCL cell lines transduced with doxycycline-inducible shRNA to knock down ALK expression were previously described<sup>32</sup>.

HEK-293T and 293 Phoenix packaging cells were obtained from DSMZ and cultured in DMEM, 10% FBS, 2% penicillin, streptomycin 5 mg ml<sup>-1</sup> and 1% glutamine.

ALK+ Ki-JK and ALK- T cell lymphoma lines were kindly provided by D. Weinstock (Dana-Farber Cancer Institute). DL-40 (ALK-negative ALCL) were maintained in IMDM + 20% FBS; Ki-JK, OCI-Ly13.2 (T cell lymphoma) and OCI-Ly12 (PTCL-NOS) were maintained in RPMI + 10% FBS; MAC2A (ALK-negative ALCL) was maintained in RPMI + 20% FBS; and DERL2 (hepatosplenic T cell lymphoma) was maintained in RPMI + 20% FBS + 100 U per ml human IL-2. ALK+ COST cell line was kindly provided by L. Lamant (Centre de Recherche en Cancérologie de Toulouse).

Immortalized EBV-transformed B lymphoblastoid cell lines were obtained from healthy controls and patients with WAS (enrolled in clinical protocol 04-09-113R) as previously described<sup>42</sup> and cultured in RPMI 1640 medium (Thermo Fisher Scientific) supplemented with 10% FBS, 2% penicillin, streptomycin 5 mg ml<sup>-1</sup> (Gibco) and 1% glutamine (Gibco).

Murine lymphoma cell lines were obtained from transgenic mice with the corresponding genotype. Briefly, at the humane endpoint mice were euthanized and tumoral thymuses were resected. Single-cell suspensions were prepared from fresh tumoral thymuses with mechanical disaggregation and were isolated by using 40- $\mu$ m nylon cell strainer (BD Biosystems). Cells were grown in RPMI and cultured for at least 4 weeks before proceeding with further experiments.

**Virus preparation and cell transduction.** Lentiviruses were produced using the third-generation production system. Briefly, 293T cell lines were cultured in DMEM with 10% FBS. Cells at 70% confluency were co-transfected with pVSVG, pCMVR8.74, pRSV-Rev and a lentiviral vector expressing the construct of interest. Medium was replenished 12 or 18 h after transfection, and the supernatant was collected after 24 and 48 h. Collected supernatants were filtered through a 0.22- $\mu$ m filter, concentrated by ultracentrifugation ( $\times 50,000g$  for 2 h) and resuspended in 500  $\mu$ l of sterile PBS. For infection,  $5 \times 10^4$  cells were infected with the prepared lentivirus along with polybrene (8  $\mu$ g ml<sup>-1</sup>), and cells with viral particles were spun down at 2,500 r.p.m. for 90 min and then incubated at 37°C overnight.

STAT3- and C/EBP $\beta$ -specific shRNAs and inducible ALK shRNA have been previously described<sup>43,44</sup>. Human Flag-WASP and Flag-WIP cDNA were obtained from A. Galy (Institut Gustave Roussy) and from Addgene, respectively. For the doxycycline-inducible system (Tet-ON), WASP and WIP cDNA were cloned into a modified pCCL vector as previously described<sup>45</sup>. SU-DHL1, JB6, DEL and Karpas-299 cell lines were co-infected with pCCL and rTA plasmids. For cell-sorting enrichment, cells were induced with 1  $\mu$ g ml doxycycline for 12 h and sorted for GFP expression on a MoFlo High-Performance Cell Sorter (DAKO Cytomation).

Retroviruses were generated by transfection of pWZL Blast vector expressing CRE-ERT2 in 293 Phoenix packaging cells. Transfected cells were incubated at 37°C for 12 or 18 h, and supernatants containing viral particles were collected at 24

and 48 h. 300  $\mu$ l retroviral supernatants were used to transduce  $5 \times 10^4$  lymphoma cells as previously described<sup>23</sup>. CRE-ERT2-transduced cells were selected using blasticidin (Calbiochem) at 25  $\mu$ g ml<sup>-1</sup> for 6 days.

**Cell lysis and immunoblotting.** Total cellular protein was extracted with GST-FISH buffer (10 mM MgCl<sub>2</sub>, 150 mM NaCl, 1% NP40, 2% glycerol, 1 mM EDTA, 25 mM HEPES pH 7.5), added with 1 mM phenylmethylsulfonyl fluoride, 10 mM NaF, 1 mM Na<sub>2</sub>VO<sub>4</sub> and protease inhibitors (Roche). Total cell lysate was cleared by centrifugation (13,000 r.p.m.) at 4°C in a microcentrifuge for 10 min and quantified using the Bio-Rad protein assay method. Protein samples were normalized based on protein concentration, denatured by addition of Laemmli buffer and boiled for 10 min. Thirty to fifty micrograms of proteins were run on sodium dodecyl sulfate-polyacrylamide gel electrophoresis under reducing conditions and transferred to nitrocellulose (GE Healthcare). Membranes were incubated with specific antibodies, detected with peroxidase-conjugated secondary antibodies (GE Healthcare) and enhanced using chemiluminescent reagent (Amersham).

The following primary antibodies were used: anti-ALK (Invitrogen, Catalog no. 35-4300), anti-human WASP (Epitomics, Clone:EP2541Y, Catalog no. 2422-1), anti-murine WASP (Cell Signaling Technology, Catalog no. 4860), anti-N-WASP (Cell Signaling Technology, Clone:30D10, Catalog no. 4848), anti-WIP (Santa Cruz Biotechnology, Clone:H-224, Catalog no. sc-25533), anti-phospho-STAT3 (Tyr705) (Cell Signaling Technology, Catalog no. 9131), anti-STAT3 (Cell Signaling Technology, Clone:79D7, Catalog no. 4904), anti-phospho-ERK (Thr202/Tyr204) (Cell Signaling Technology, Catalog no. 9101), anti-ERK (Cell Signaling Technology, Catalog no. 9102), anti-phospho-AKT (Ser473) (Cell Signaling Technology, Clone:D9E, Catalog no. 4060), anti-AKT (Cell Signaling Technology, Clone:11E7, Catalog no. 4685), anti-phospho-JNK (Thr183/Tyr185) (Cell Signaling Technology Clone:G9, Catalog no. 9255), anti-JNK (Cell Signaling Technology, Catalog no. 9252), anti-CDC42 (BD Transduction Laboratory, Catalog no. 610929), anti-C/EBP $\beta$  (Santa Cruz Biotechnology, Clone:C-19, Catalog no. sc-150), anti-Cleaved Caspase 3 (Asp175) (Cell Signaling Technology, Catalog no. 9661), anti-phospho S6 (Ser235/236) (Cell Signaling Technology, Clone:D57.2.2E, Catalog no. 4858) and anti-S6 (Cell Signaling Technology, Clone:54D2, Catalog no. 2317), HSP90 (Santa Cruz Biotechnology, Clone:H114, Catalog no. sc-7947), anti-ZAP70 (Millipore, Clone:2F3.2, Catalog no. 05-253) anti-GFP (Invitrogen, Catalog no. A-11122), anti-Actin (Sigma-Aldrich, Catalog no. A2066).

**Histology, immunohistochemistry and immunofluorescence.** For histology, tissue samples were formalin-fixed and paraffin embedded, cut into 4- $\mu$ m-thick sections and stained with H&E.

For immunohistochemistry, formalin-fixed sections were de-waxed in xylene and dehydrated by passage through graded alcohols to water; sections were microwaved in citrate buffer pH 6 for 15 min and then transferred to PBS. Endogenous peroxidase was blocked using 1.6% hydrogen peroxide in PBS for 10 min followed by washing in distilled water. Normal serum diluted to 10% in 1% bovine serum albumin (BSA) was used to block nonspecific staining.

The slides were then incubated for 1 h with the following primary antibodies: anti-WASP (Epitomics), anti-WIP (Clone:H-224, Santa Cruz Biotechnology), anti-ALK (Clone: 18-0266, Zymed); anti-cleaved caspase 3 (Cell Signaling Technology), anti-murine Ki-67 (AbCam, Clone:SP6, Catalog no. ab16667) and anti-human Ki-67 (DAKO, Clone:MIB-1, Catalog no. M7240). After washing, sections were incubated with biotinylated secondary goat antibody to rabbit IgG and visualized with the EnVision system (Dako).

For immunofluorescence, cells were plated on glass coverslips pretreated with fibronectine (10  $\mu$ g ml<sup>-1</sup> PBS) at 37°C for 1 h and incubated overnight in fresh medium. Samples were fixed in 4% paraformaldehyde at room temperature for 10 min and permeabilized with 0.3% Triton X-100 for 5 min. Coverslips were incubated with 3% BSA for 1 h at room temperature and then stained with phycoerythrin-conjugated phalloidin (1/500, Sigma) and HOECHST (300 ng ml<sup>-1</sup>, Sigma). Coverslips were mounted on microscope slides using anti-fading solution and viewed using a Leica photomicroscope. Images were acquired at room temperature by means of HXC PL APO  $\times 100/1.40$  OIL (Leica, Heidelberg, Germany) and analyzed by DM LM Leica software. Cell dimension has been measured using ImageJ software.

The slides were reviewed by experienced hematopathologists, and quantification of the levels of WASP and WIP expression was performed selectively in multiple areas where lymphoma cells were clearly enriched. This selection was achieved by comparing the areas on serial sections stained with the following markers: ALK for ALK+ ALCL, CD30 for ALK- ALCL, CD10 for AITL. When a marker was not available (such as loss of a particular T cell antigen) for PTCL-NOS, NK/T cell lymphoma and hepatosplenic  $\gamma\delta$  T cell lymphoma, the selection of the areas with enriched lymphoma cells was based on morphologic criteria, such as a cluster of atypical cells or invasion of specific structures such as vessels in NK/T cell lymphoma or sinusoids in hepatosplenic  $\gamma\delta$  T cell lymphoma. The quantification of WASP and WIP expression levels was achieved by comparison with an internal control constituted by normal B and T lymphocytes.

**qRT-PCR analysis.** Total RNA was extracted from cells using TRIzol solution (Invitrogen), followed by cDNA preparation from 1  $\mu$ g of total RNA. cDNA

products were quantified by real-time PCR using SYBR Green Supermix (Bio-rad) on Bio-Rad iCycler iQ Real-Time PCR Detection System. Normalization was performed against the housekeeping human acidic ribosomal protein (*HuPO*) or Actin according to the formula  $2^{-\Delta\Delta C_t}$ , where the  $\Delta C_t = \frac{1}{4} C_t$  (threshold cycle) gene of interest  $- C_t$  internal control, as indicated by the manufacturer.

WASP-specific primers: forward 5'-GAAACGCTCAGGGAAGAAGA-3', reverse 5'-CTGCCCTGGAGAAACGACTC-3';  
WIP-specific primers: forward 5'-ACAGGATAATGATTCTGGAGG-3', reverse 5'-CTGGAGAAGGCACAGGAAAC-3';  
HuPO-specific primers: forward 5'-GCTTCTGGAGGGTGTCC-3', reverse 5'-GCTTCTGGAGGGTGTCC-3';  
Actin-specific primers: forward 5'-ACGAGCCCCCTGAAC-3', reverse 5'-CAGGTCCAGACGCAGGATGGC-3';  
LAT-specific primers forward 5'-ACAGTGTGGCGAGCTACG-3', reverse 5'-CGTTCAGTAATCATCAATGG-3'

**DNA demethylation.** ALK+ ALCL cell lines (TS, SU-DHL1 and JB6) were plated in a six-well plate ( $5 \times 10^5$  cells per ml), treated with 5  $\mu$ M of the methyltransferase inhibitor 5-aza-2-deoxycytidine (Sigma). Cells were washed twice in PBS and collected at 0, 48, 72, 96 and 144 h after the treatment. Cells were collected for western blot and qRT-PCR assays.

ZAP70 and LAT were used as positive controls for western blot and qRT-PCR, respectively, as previously reported<sup>30</sup>.

**Chromatin immunoprecipitation.** JB6 and SU-DHL1 cells were fixed in 1% formaldehyde (Sigma-Aldrich, F8775) for 10 min at 37 °C. Subsequently, glycine was added to 125 mM and incubated at 37 °C for 5 min at 37 °C. Next, cells were pelleted and washed twice with cold PBS. Pellets were stored at  $-80$  °C until use.

Nuclei from 10M cells per ChIP-seq were extracted, and chromatin was sonicated with a Covaris sonicator. Immunoprecipitation reactions were performed overnight with anti-STAT3 (Cell Signaling Technology, Clone:124H6, Catalog no. 9139) or anti-C/EBP- $\beta$  (Abcam, Clone:E299, Catalog no. ab32358) antibodies. The next morning, antibodies and chromatin were captured using Protein G Dynabeads (Thermo Fisher). Material was washed, eluted and treated with RNase A (Roche 11 119 915 011) for 30 min at 37 °C and Proteinase K (Life Technologies 100005393) for 3 h at 65 °C. DNA was extracted using SPRI beads (Beckman Coulter Agencourt AMP Xpure).

H3K4me3, H3K27ac and H3K27me3 profiles on Jurkat<sup>46-48</sup> and GM12878<sup>49</sup> cell lines were obtained from public databases, including ENCODE.

**Library preparation and sequencing.** Library preparation of ChIP-seq DNA was performed using the Ultra II Library Prep Kit (NEB E7103L) and Multiplex Oligos for Illumina (NEB E7335L) and sequenced on an Illumina Nextseq 500 (75 base pairs single end).

**ChIP-seq data processing.** ChIP-seq samples were sequenced with the Illumina NextSeq technology, and output data were demultiplexed and converted to FASTQ format using the bcl2fastq software tool. Read quality was assessed by FASTQC, and ChIP-seq reads were aligned to the hg19 genome with Bowtie2 v2.29 in the -k 1 reporting mode<sup>50</sup>. Output BAM files were converted into BigWig track files using the 'callpeak' function of MACS2 v2.1.1 with the '-B -SPMR' option followed by the use of the BEDTools<sup>51</sup> 'sort' function and the UCSC utility 'bedgraphToBigWig'<sup>52</sup>, and the tracks were visualized in IGV v2.4.3. Narrow peaks were called with the MACS2 v2.1.1 software using input as controls and a *q* value cutoff of 0.001<sup>53</sup>. Metaplots and heatmaps were generated using ngsplot v2.61<sup>54</sup>.

**Gene-expression profiling.** Total RNA was extracted from primary *NPM-ALK/Wasp*<sup>+/+</sup> or *NPM-ALK/Wasp*<sup>-/-</sup> lymphoma using TRIzol reagent (Invitrogen) and purified using the RNeasy total RNA Isolation Kit (Qiagen). GeneChip Mouse Gene 1.0ST Array from Affymetry was used for profiling.

**Apoptosis assay and cell cycle analysis.** Cre-ERT2-transduced murine cells were grown in six-well plates after treatment with 10 nM 4-hydroxytamoxifen (4OHT; Sigma) for 4 h. At 0, 24 and 48 h after the treatment, cells were stained with 200 nM tetramethylrodamine methyl-ester (TMRM) for 15 min in dark and washed twice in PBS, and the percentage of apoptotic cells was measured by flow cytometry (BD FACSCALIBUR) using the CellQuest Program.

For cell cycle analysis, the DNA content was determined with propidium iodide staining. SU-DHL1 and Karpas-299 cell lines either expressing WASP- and WIP-inducible vector or the GFP control were treated for 168 h with doxycycline (1  $\mu$ g ml<sup>-1</sup>), cells were washed with PBS, resuspended in citric acid buffer (0.05 M Na<sub>2</sub>HPO<sub>4</sub>, 25 mM sodium citrate and 0.1% Triton X-100 (pH 7.3)), treated with RNase (0.25 mg ml<sup>-1</sup>) and then stained with propidium iodide (50  $\mu$ g ml<sup>-1</sup>) for 15 min at 37 °C in the dark. The G<sub>1</sub> and S/G<sub>2</sub>-M cell fractions were calculated for the nonapoptotic cell population only.

**Cell viability assay.** Cell viability assay on human ALK+ ALCL cell lines was performed using CellTiter-Glo (Promega), according to manufacturer's instruction.

Briefly, cells were seeded into white walled 96-well plates (three wells per sample) in the presence or absence of treatment (doxycycline, 4-hydroxytamoxifen or trametinib). CellTiter-Glo reagent was added to each well, and luminescence output data were taken at 0, 24, 48 and 72 h by GloMax-Multi Detection System (Promega). Trametinib was purchased from Selleckem, diluted in DMSO and used at the indicated concentrations.

**Drug-sensitivity assay.** Drug-sensitivity assays were performed as previously described<sup>55</sup>. Briefly, cells ( $2 \times 10^3$ ) were seeded in 96-well plates in RPMI complete medium. The following day, cells were treated with selumetinib (Selleckchem, Catalog no. S1008), trametinib (Selleckchem Catalog no. S2673), crizotinib (kindly provided by Pfizer), MEK162 (Selleckchem Catalog no. S7007) or PD0325901 (Selleckchem Catalog no. S1036) using a ten-point dose titration scheme from 1 nM to 10  $\mu$ M or from 1 nM to 1  $\mu$ M. After 72 h, cell viability was assessed using colorimetric MTS assay (CellTiter 96 Aqueous Non-Radioactive Cell Proliferation Assay (MTS) Powder, Promega). Absolute inhibitory concentration values were calculated using four-parameter logistic curve fitting. All experimental points were a result of three to six replicates and all experiments were repeated at least three times. The data was graphically displayed using GraphPad Prism 7 for Windows (GraphPad Software). Each point (mean  $\pm$  s.d.) represents growth of treated cells compared to untreated cells. The curves were fitted using a nonlinear regression model with a sigmoidal dose response.

**Measurement of GTP-bound CDC42.** To measure the amount of GTP-bound CDC42, cells were plated at the same concentration in six-well plates and incubated in RPMI medium overnight. Cells were collected and lysed as previously described. CDC42 activity was determined using CDC42 G-LISA assay kit in accordance with the manufacturer's instructions (Cytoskeleton Inc.). Briefly, cells were collected and washed three times in ice-cold PBS on cold centrifuge, and protein lysates were transferred to ice-cold 1.5-ml centrifuge tubes and clarified by centrifuging at 10,000 r.p.m. for 2 min and then were immediately snapped frozen in liquid nitrogen. Protein concentrations were determined using the Precision Red Advance Protein Assay (Cytoskeleton), and 1.0 mg ml<sup>-1</sup> protein was used for the GTPase activation assay. Fifty microlitres of protein lysate were added to a precoated 96-well plate, and then the plate was washed and antigen-presenting buffer was added, which was followed by primary and secondary antibodies. The reaction was detected using horseradish peroxidase detection reagent followed by the stop buffer. The plate was read immediately by measuring absorbance at 490 nm on a microplate spectrophotometer.

Human ALCL cell lines, stably transfected with Tet-ON WASP & WIP and the empty control Tet-ON GFP plasmid, were treated with doxycycline (1  $\mu$ g ml<sup>-1</sup>). After 48 h, cells were lysed, and GTP-bound CDC42 was immunoprecipitated using CDC42 Activation Assay Kit (NewEast Biosciences). Quantification was performed by densitometric analysis of the western blot bands.

**Flow cytometry.** Six-week-old mice were euthanized, and thymuses were resected and used for flow cytometry analysis. Single-cell suspensions were prepared from fresh prethymal thymuses with mechanic disaggregation and isolated by using 40- $\mu$ m nylon cell strainers (BD Biosystems). Cells were resuspended in PBS and stained with PE-anti-mouse CD4 (clone GK1.5; Miltenyi Biotec) and PerCP-anti-mouse CD8a (clone 53-6.7; BioLegend) for 15 min, and then were washed and resuspended in PBS. Cells were then acquired in a FACSCalibur flow cytometer (BD Bioscience) and analyzed using the FlowJo software.

For co-culture assays, SU-DHL1 and JB6 cell lines either expressing WASP and WIP inducible vector or the GFP control were mixed 1:1 with parental cells, the percentage of GFP positive cells was followed over time for 40 days by flow cytometry.

**T cell purification, ex vivo activation and proliferation analysis.** Untouched T cells were isolated from spleens of WASP- and WIP-deficient mice and wild-type mice by immunomagnetic depletion of B cells, monocytes/macrophages, natural killer cells, dendritic cells, erythrocytes and granulocytes.

Briefly, spleens were collected, placed on ice, washed in PBS to remove residual blood, cut into small pieces, crushed and physically dissociated using a Falcon cell strainer and subjected to hypotonic lysis of erythrocytes. Cells were resuspended in isolation buffer (PBS supplemented with 0.1% BSA and 2 mM EDTA). All non-T cells were depleted with a mixture of rat monoclonal IgG antibodies against non-T cells ('Antibody mix': anti mouse CD45R, CD11b, Ter-119 and CD16/CD32; Invitrogen) combined with Mouse Depletion Dynabeads (4.5  $\mu$ m diameter beads coated with a polyclonal sheep anti-rat IgG antibody; Invitrogen) following the manufacturer's instructions.

Isolated mouse T cells, bead- and antibody-free, were activated by adding Dynabeads Mouse T-Activator CD3/CD28 (polyclonal activation; Invitrogen).

For T cell proliferation analysis, purified and activated T cells ( $1 \times 10^6$  cells) were plated in a six-well plate and cultured at 37 °C in RPMI 1640 medium supplemented with 15% FBS, 2% penicillin, streptomycin 5 mg ml<sup>-1</sup> and 50 mM 2-mercaptoethanol for 48 h. Cells were then collected for CellTiter-Glo analysis (Promega) following the manufacturer's instructions.

For western blot analysis, cells were collected after 15 min of incubation with the cocktail of CD3/CD28 beads, centrifuged and washed with cold PBS for protein extraction.

**Statistical analysis.** Statistical analysis was performed with GraphPad PRISM 7.0 software. *P* values were calculated by using the unpaired, two-tailed Student's *t*-test with Welch's correction as indicated in each figure legend. Kaplan–Meier analysis for survival curve was performed with GraphPad Prism 7, and *P* values were determined with a log-rank (Mantel–Cox) test.

**Reporting Summary.** Further information on research design is available in the Nature Research Reporting Summary linked to this article.

### Data availability

The Gene Expression Omnibus repository accession number for the gene expression profiling data from wild type and *Wasp*<sup>-/-</sup> mice is [GSE102889](https://www.ncbi.nlm.nih.gov/geo/query/acc.cgi?acc=GSE102889) (token: gzelisgodjkdxtq); and for ChIP-seq data, the accession number is [GSE117164](https://www.ncbi.nlm.nih.gov/geo/query/acc.cgi?acc=GSE117164) (token: chupqsgklxivtox). Gene-expression profiling data for human T cell lymphoma have been deposited with Gene Expression Omnibus repository accession number [GSE65823](https://www.ncbi.nlm.nih.gov/geo/query/acc.cgi?acc=GSE65823) (ref. <sup>13</sup>).

### References

41. Wu, X. et al. Cdc42 controls progenitor cell differentiation and beta-catenin turnover in skin. *Genes Dev.* **20**, 571–585 (2006).
42. Facchetti, F. et al. Defective actin polymerization in EBV-transformed B-cell lines from patients with the Wiskott–Aldrich syndrome. *J. Pathol.* **185**, 99–107 (1998).
43. Martinengo, C. et al. ALK-dependent control of hypoxia inducible factors mediates tumor growth and metastasis. *Cancer Res.* **74**, 6094–106 (2014).
44. Piva, R. et al. Functional validation of the anaplastic lymphoma kinase signature identifies CEBPB and BCL2A1 as critical target genes. *J. Clin. Invest.* **116**, 3171–3182 (2006).
45. Ceccon, M. et al. Excess of NPM-ALK oncogenic signaling promotes cellular apoptosis and drug dependency. *Oncogene* **35**, 3854–3865 (2016).
46. Orlando, D. A. et al. Quantitative ChIP-seq normalization reveals global modulation of the epigenome. *Cell reports* **9**, 1163–1170 (2014).
47. Mansour, M. R. et al. Oncogene regulation. An oncogenic super-enhancer formed through somatic mutation of a noncoding intergenic element. *Science* **346**, 1373–1377 (2014).
48. Manser, M. et al. ELF-MF exposure affects the robustness of epigenetic programming during granulopoiesis. *Sci. Rep.* **7**, 43345 (2017).
49. Thurman, R. E. et al. The accessible chromatin landscape of the human genome. *Nature* **489**, 75–82 (2012).
50. Langmead, B. & Salzberg, S. L. Fast gapped-read alignment with Bowtie 2. *Nat. Methods* **9**, 357–359 (2012).
51. Quinlan, A. R. & Hall, I. M. BEDTools: a flexible suite of utilities for comparing genomic features. *Bioinformatics* **26**, 841–842 (2010).
52. Kuhn, R. M., Haussler, D. & Kent, W. J. The UCSC genome browser and associated tools. *Brief. Bioinform.* **14**, 144–161 (2013).
53. Zhang, Y. et al. Model-based analysis of ChIP-seq (MACS). *Genome. Biol.* **9**, R137 (2008).
54. Shen, L., Shao, N., Liu, X. & Nestler, E. ngs.plot: quick mining and visualization of next-generation sequencing data by integrating genomic databases. *BMC Genomics* **15**, 284 (2014).
55. Ambrogio, C. et al. Kras dimerization impacts MEK inhibitor sensitivity and oncogenic activity of mutant KRAS. *Cell* **172**, 857–868 e815 (2018).

## Life Sciences Reporting Summary

Nature Research wishes to improve the reproducibility of the work that we publish. This form is intended for publication with all accepted life science papers and provides structure for consistency and transparency in reporting. Every life science submission will use this form; some list items might not apply to an individual manuscript, but all fields must be completed for clarity.

For further information on the points included in this form, see [Reporting Life Sciences Research](#). For further information on Nature Research policies, including our [data availability policy](#), see [Authors & Referees](#) and the [Editorial Policy Checklist](#).

Please do not complete any field with "not applicable" or n/a. Refer to the help text for what text to use if an item is not relevant to your study. For final submission: please carefully check your responses for accuracy; you will not be able to make changes later.

### ► Experimental design

#### 1. Sample size

Describe how sample size was determined.

In the transgenic mice experiment more than 30 mice for each genotype has been used. This large number of mice was achieved in several years of breeding. The only exception was the NPM-ALK, WASP<sup>-/-</sup> CDC42f/f, CD4-CRE genotype that showed short lifespan and therefore was not useful to determine lymphoma incidence. No sample size calculation was predetermined. All mice were bred to perform various experiments required by the project and survival curves were then calculated by collecting the total number of mice for each genotype.

#### 2. Data exclusions

Describe any data exclusions.

Each mouse was evaluated by autopsy for lymphoma. Mice that died for other causes without evidence of lymphoma were excluded from survival curves. No exclusion criteria were pre-established.

#### 3. Replication

Describe the measures taken to verify the reproducibility of the experimental findings.

All experiments have been repeated in technical and/or biological triplicates as indicated in the Figure legends. All attempts at replication were successful.

#### 4. Randomization

Describe how samples/organisms/participants were allocated into experimental groups.

All mice were randomly allocated in each group. For WASP deficient mice, because WASP is on the X chromosome, WASP<sup>-/-</sup> females and WASP<sup>-/-</sup> males were equally distributed between experimental groups.

#### 5. Blinding

Describe whether the investigators were blinded to group allocation during data collection and/or analysis.

No blinded group allocation was used during the experiment procedures. Blinding was not relevant to this study as each experiment was associated with proper controls. For xenografts experiments with human lymphoma, for ethical reason the minimum number of mice to provide statistical values was determined based on previous experimental data and published articles.

Note: all in vivo studies must report how sample size was determined and whether blinding and randomization were used.

## 6. Statistical parameters

For all figures and tables that use statistical methods, confirm that the following items are present in relevant figure legends (or in the Methods section if additional space is needed).

n/a Confirmed

- The exact sample size ( $n$ ) for each experimental group/condition, given as a discrete number and unit of measurement (animals, litters, cultures, etc.)
- A description of how samples were collected, noting whether measurements were taken from distinct samples or whether the same sample was measured repeatedly
- A statement indicating how many times each experiment was replicated
- The statistical test(s) used and whether they are one- or two-sided  
*Only common tests should be described solely by name; describe more complex techniques in the Methods section.*
- A description of any assumptions or corrections, such as an adjustment for multiple comparisons
- Test values indicating whether an effect is present  
*Provide confidence intervals or give results of significance tests (e.g.  $P$  values) as exact values whenever appropriate and with effect sizes noted.*
- A clear description of statistics including central tendency (e.g. median, mean) and variation (e.g. standard deviation, interquartile range)
- Clearly defined error bars in all relevant figure captions (with explicit mention of central tendency and variation)

See the web collection on [statistics for biologists](#) for further resources and guidance.

## ► Software

Policy information about [availability of computer code](#)

### 7. Software

Describe the software used to analyze the data in this study.

ImageJ v. 1.50i; iCycler iQ Software v. 3.1; CellQues Pro v6.0; FlowJo v10.5; GloMax Microplate Luminometer Software v1.9.3; GraphPad Prism v6.05; Leica Application Suite X; Demultiplexing: bcl2fastq; Quality Control: FASTQC; Read Alignment: Bowtie2 version 2.29; Peak Calling: MACS2 version 2.1.1; Track Generation: MACS2 version 2.1.1 “callpeak” function with “-B --SPMR” option, BEDTools “sort” function, the UCSC utility “bedgraphToBigWig”; Track Visualization: IGV version 2.4.3; Metaplot and Heatmap Generation: ngsplot version 2.6.1

For manuscripts utilizing custom algorithms or software that are central to the paper but not yet described in the published literature, software must be made available to editors and reviewers upon request. We strongly encourage code deposition in a community repository (e.g. GitHub). *Nature Methods* [guidance for providing algorithms and software for publication](#) provides further information on this topic.

## ► Materials and reagents

Policy information about [availability of materials](#)

### 8. Materials availability

Indicate whether there are restrictions on availability of unique materials or if these materials are only available for distribution by a third party.

Mouse models and primary derived cells lines of all genotypes are available for distribution without restrictions.



## 9. Antibodies

Describe the antibodies used and how they were validated for use in the system under study (i.e. assay and species).

We validated anti-Wasp and anti-Wip antibodies used in the study by internal controls such as comparing WT to knock-out or knock-down cells in WB blot and immunohistochemistry. Flow cytometry antibodies were validated by using corresponding negative cells for each stains.

For WB and immunohistochemistry, the antibodies were purchased by qualified vendors that provided a validation on the manufacturer's website.

The following antibodies were used:

anti-ALK 1:2000(Invitrogen, Catalog#:35-4300), anti-human WASP 1:2000 (Epitomics, Clone:EP2541Y, Catalog#:2422-1), anti-murine WASP 1:2000 (Cell Signaling Technology, Catalog#:4860), anti-N-WASP 1:1000 (Cell Signaling Technology, Clone:30D10, Catalog#:4848), anti-WIP 1:2000 (Santa Cruz Biotechnology, Clone:H-224, Catalog#:sc-25533), anti-phospho-STAT3 (Tyr705) 1:2000 (Cell Signaling Technology, Catalog#:9131), anti-STAT3 1:2000 (Cell Signaling Technology, Clone:79D7, Catalog#:4904), antiphospho-ERK (Thr202/Tyr204) 1:2000 (Cell Signaling Technology, Catalog#:9101), anti-ERK 1:2000 (Cell Signaling Technology, Catalog#:9102), anti-phospho-AKT (Ser473) 1:1000 (Cell Signaling Technology, Clone:D9E, Catalog#:4060), anti-AKT 1:2000 (Cell Signaling Technology, Clone:11E7, Catalog#:4685), anti-phospho-JNK (Thr183/Tyr185) 1:1000 (Cell Signaling Technology, Catalog#:9255), anti-JNK 1:2000 (Cell Signaling Technology, Catalog#:610929), anti-C/EBP $\beta$  1:1000 (Santa Cruz Biotechnology,Clone:C-19, Catalog#:sc-150), anti-Cleaved Caspase-3 (Asp175) 1:1000 (Cell Signaling Technology,Catalog#:9661), anti-phospho S6 1:1000 (Cell Signaling Technology, clone D57.2.2E, Catalog#:4858), anti-S6 1:1000 (Cell Signaling Technology, clone 54D2, Catalog#:2317), anti-HSP90 1:2000 (Santa Cruz Biotechnology, #H114), anti-ZAP70 1:1000 (Millipore, Clone:2F3.2, Catalog#:05-253), anti-GFP 1:2000 (Invitrogen, Catalog #:A-11122), anti-Actin 1:4000 (Sigma-Aldrich, Catalog#:A2066)

## 10. Eukaryotic cell lines

a. State the source of each eukaryotic cell line used.

Human ALK+ ALCL cell lines (SU-DHL1, Karpas-299, DEL, SUP-M2 and L82) and ALK- cell lines (MAC-1 and Jurkat) ALCL cell lines were obtained from DSMZ (German collection of Microorganisms and Cell Cultures).

HEK-293T and 293 Phoenix packaging cells were obtained from DSMZ.

ALK-positive Ki-JK cell line and ALK negative T cell lymphoma lines (DL-40, OCI-Ly13.2, OCI-Ly12, MAC2A and DERL2) were kindly provided by Dr. David Weinstock (Dana-Farber Cancer Insitute, Boston, USA).

ALK-positive COST cell line was kindly provided by Dr. Laurence Lamant (Centre de Recherche en Cancérologie de Toulouse, France).

ALK-positive (TS and JB6) and ALK-negative FePD cell lines were kindly provided by Dr. Giorgio Inghirami (Department of Pathology and Laboratory Medicine, Weill Cornell Medicine, New York, NY, USA)

b. Describe the method of cell line authentication used.

Stock of cells lines were immediately generated after purchase. For experiments, cell lines were never kept for more than 3 consecutive months in culture, if needed for longer time a new stock was used. For some cells lines we also further authenticated them by sequencing of the mutations present in the p53 gene which are unique for each NPM-ALK cell line.

c. Report whether the cell lines were tested for mycoplasma contamination.

Cell lines were tested for mycoplasma monthly. If cells resulted positive for contamination, they were treated with mycoplasma removal agents until three consecutive PCR tests were negative.

d. If any of the cell lines used are listed in the database of commonly misidentified cell lines maintained by [ICLAC](#), provide a scientific rationale for their use.

No commonly misidentified cell lines has been used

## ► Animals and human research participants

Policy information about [studies involving animals](#); when reporting animal research, follow the [ARRIVE guidelines](#)

### 11. Description of research animals

Provide all relevant details on animals and/or animal-derived materials used in the study.

All the animals in the studies are mice, all the transgenic mice were maintained in C57BL/6 background; male and female mice were randomly selected. Primary lymphoma cell lines with different genotypes were immortalized from mice spontaneously without any type of genetic manipulation.

Pre-tumoral thymuses were collected from 4-6 weeks old mice; tumoral thymuses were collected from 12-16 weeks old mice.

For xenograft experiments NSG immunocompromised mice were used. Mice of 8  $\pm$  2 weeks of age and randomly sorted by sex were used.

## 12. Description of human research participants

Describe the covariate-relevant population characteristics of the human research participants.

This study did not involve human research